NRL Report 7659

A Five-Channel (2-kW-PEP) 2 to 30 MHz Distribution System

HAROLD D. MURRAY, DENIS Q. ARNESEN, AND CHARLES E. HOBBIS

Communication Systems Branch
Communications Sciences Division

December 21, 1973

NAVAL RESEARCH LABORATORY
Washington, D.C.

Approved for public release; distribution unlimited.

CONTENTS

Abstract ii

INTRODUCTION 1

EXISTING SHIPBOARD DISTRIBUTION SYSTEMS 1

SELF-CONTAINED SELECTIVE DISTRIBUTION SYSTEM (SSDS) . . . 4

Objectives and Design Considerations 4
Experimental Design 6
Performance Characteristics 10

SYSTEM CONSIDERATIONS 17

Automation 17
Provision for Auxiliary Antenna 18
Installation 18
Antenna Requirements 19
Companion Receiving System 19

CONCLUSION 22

RECOMMENDATION 22

ACKNOWLEDGMENT 22

APPENDIX A — Evolution of the Resonator Inductor 23

APPENDIX B — Design of the Resonator and the Combiner 33

ABSTRACT

The concept of a radio-frequency distribution system customized to the special requirements and constraints of ships having five transmitters or less has been investigated. The analysis, experimental design, and measurements of the performance of an experimental model of one channel of the system has successfully been completed. When fully implemented the system will provide for the simultaneous operation of five transmitters in the 2 to 30 MHz frequency range into two broadband antennas in a single systems package. A program should be initiated to develop a complete self-contained selective distribution system as an engineering model of the system whose design was proven by the present investigation.

Manuscript submitted September 18, 1973.

A FIVE-CHANNEL (2-kW-PEP) 2 TO 30 MHz DISTRIBUTION SYSTEM

INTRODUCTION

The typical U.S. Navy shipboard environment creates severe restrictions on the usable sites available for communication antennas. For maximum use of the antennas, radio-frequency (RF) distribution systems are normally included in an installation. The problem is further compounded by the requirement to simultaneously transmit and receive RF energy from the confined area of the shipboard platform. In the shipboard environment most of the required isolation between transmitter and receiver must be provided by the RF distribution system.

The RF distribution system consists of the multicouplers, preselectors, tuners, couplers, and patch panels that provide the transition between the transmitter or receiver equipment and the antenna. The RF distribution system is one of the key ingredients that determines the shipboard electromagnetic compatability characteristics.

The shipboard distribution system must, upon demand and in real time, establish the RF path (channel) between transmitter or receiver equipment and the antenna. The distribution system must not introduce excessive insertion losses, place undue restriction on operations, or be disruptive to other existing circuits. Frequently, the system must cope with an intolerable situation as to the number of RF equipments and the assignments of operating frequencies. As a practical matter, however, many compromises must be accepted in the performance of distribution systems. The number of RF paths (channel capacity), insertion loss, and isolation are interrelated characteristics and largely depend on the maximum Q that can be achieved in resonant circuitry, which is proportional to the physical size. The resonant circuitry is typically contained in the transmitter and receiver multicoupler portions of the distribution system.

EXISTING SHIPBOARD DISTRIBUTION SYSTEMS

The most recently developed general-purpose shipboard multicouplers for operation with 2 to 30 MHz transmitters are designated AN/SRA-56, -57, and -58. These multicouplers are manually tuned and are rated 2 kW PEP (peak envelope power) and 1 kW rms. Figure 1 shows a system arrangement of this series of multicouplers, together with four high-frequency-band transmitters and three broadband antennas. Each multicoupler and broadband antenna combination operates over a limited portion of the HF band: 2 to 6 MHz, 4 to 12 MHz, and 10 to 30 MHz for the AN/SRA-56, -57, and -58 respectively. A patch panel is needed to switch control and interlock functions as well as the

RF outputs to permit the transmitters to be used with any of the three multicouplers. Figure 2 shows a system arrangement in which the same transmitters could be accommodated using automatically tuned multicouplers developed for the AN/SRC-16 communication system. Two cabinets of multicouplers and three broadband antennas are required. The 0A4625/SRC-16 multicoupler provides four channels in the 2 to 6 MHz band and requires a 2 to 6 MHz broadband antenna. The 0A4624/SRC-16 multicoupler provides four channels, each of which can be tuned in the 6 to 30 MHz range. The 6 to 30 MHz band is split at 15 MHz, and separate broadband antennas for the 6 to 15 and 15 to 30 MHz ranges are required. Switching is provided to permit none, two, or four of the 0A4624/SRC-16 multicoupler channels to be operated into either of the 6 to 15 MHz or 15 to 30 MHz broadband antennas. Each 2 to 30 MHz transmitter has access to each channel of both multicouplers by means of the switching matrix contained within the 0A4624/SRC-16 cabinet.

To use the systems of Figs. 1 and 2 most efficiently, a separate channel for each transmitter must be provided in each multicoupler. Of the available multicoupler channel capacity at least two-thirds of the system of Fig. 1 and half of the system of Fig. 2 is idle at any given time.

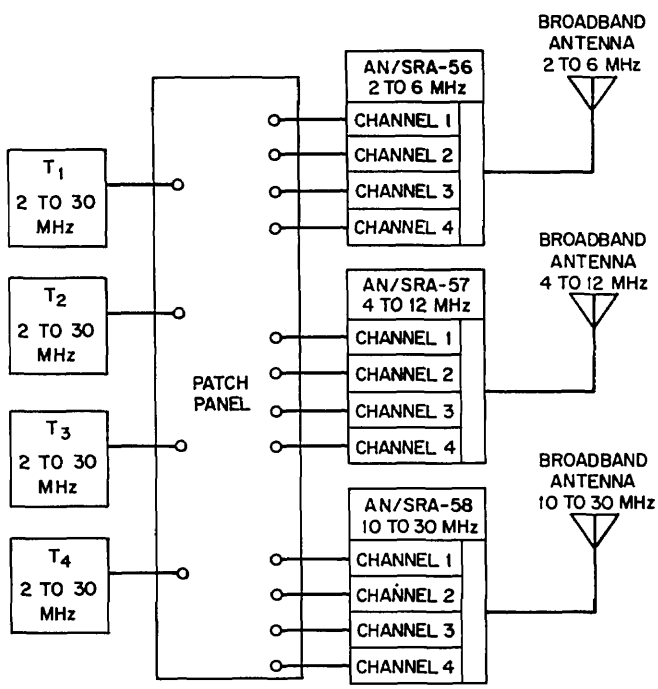

Fig. 1 — Small-ship distribution-system arrangement using current Navy manually operated multicouplers (T_1 = transmitter 1, etc.)

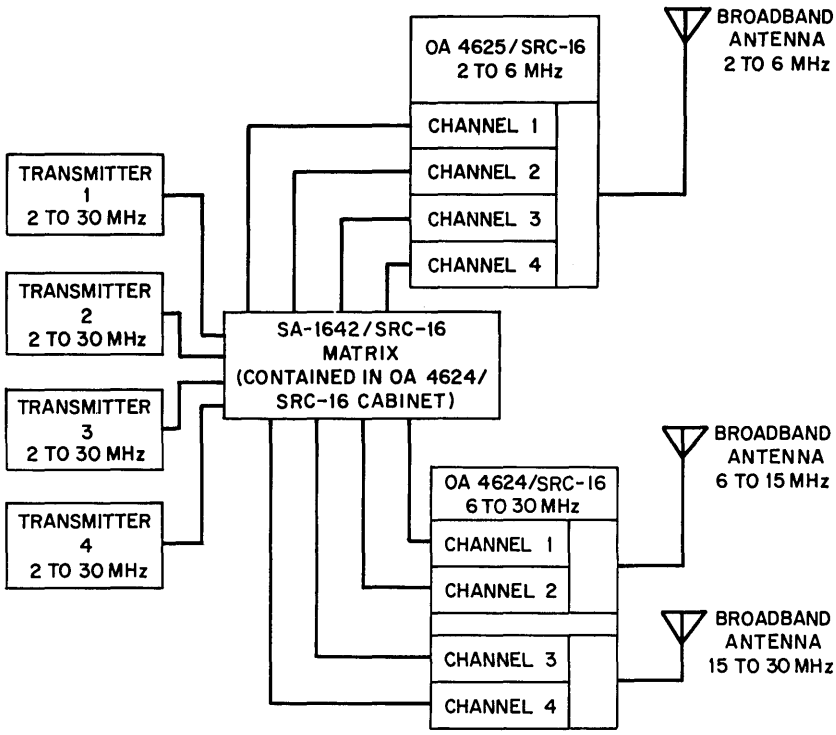

Fig. 2 — Small-ship distribution-system arrangement using current Navy automatically tuned multicouplers

The performance of the AN/SRA-56 and SRC-16 series multicouplers is an improvement over older equipments such as the AN/SRA-13 series but physically are larger. Consequently the newer equipments are being installed aboard new-construction ships and on older ships during major overhauls when the ship has sufficient space. Installation aboard older smaller ships (DE, DD, etc.) is not practical, because space to locate one or more multicoupler cabinets does not exist in the radio-transmitter compartment and topside space is not available to erect three separate broadband antennas having acceptable VSWR characteristics. Installation of only one of the new equipments to cover a difficult frequency band such as 2 to 6 MHz, is usually not feasible without overhaul to get more space.

The RF distribution system (transmit) for ships having four or five 2 to 30 MHz transmitters continues to typically consist of one multicoupler (AN/SRA-13) and broadband antenna combination operating in the 2 to 6 MHz range supplemented by several 35-foot base-tuned whips that can operate over the full 2 to 30 MHz range. The typical system arrangement as shown in Fig. 3 gives unsatisfactory performance primarily because of inadequate system isolation. For the older designed AN/SRA-13 the channel isolation is insufficient at frequency separations of less than approximately 10 percent. Existing Navy-type base tuners are designed to provide impedance matching but do not provide adequate isolation performance. The systems of Figs. 1 and 3 are dependent on a manually operated cable-type patch panel which is expensive to install, consumes valuable space, and requires excessive maintenance. Frequent mechanical stress to the cable plugs during routine patching eventually causes intermittences and failure of the connection. To

reassemble or replace a connector is time consuming and requires considerable skill and care by the technician. Mistakes in patching are easily made by an operator, causing a delay in bringing up a circuit or possibly damaging equipment. The patch panel is considered to be one of the most troublesome parts of the conventional distribution system.

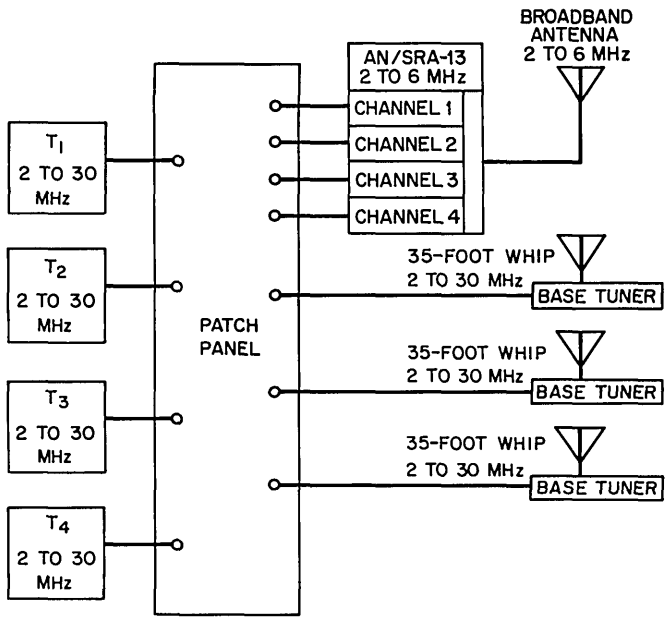

Fig. 3 — Typical small-ship distribution system

An improved RF distribution system satisfying the requirements of a ship with four 2 to 30 MHz transmitters is shown in Fig. 4. Each of the four transmitters is dedicated to a particular channel. Since each channel can be internally configured to operate over the 2 to 30 MHz frequency range, a patch panel is not required for RF signal transfer or control/interlock functions. Operation of each channel into either of two broadband antennas that collectively cover the 2 to 30 MHz band is accomplished by means of a dual-output combining network.

SELF-CONTAINED SELECTIVE DISTRIBUTION SYSTEM

Objectives and Design Considerations

The function of each channel of the SSDS is to transfer energy efficiently between the associated transmitter and antenna at the discrete channel operating frequency and to provide the necessary isolation at the operating frequencies of the other channels. The performance of the SSDS is determined by the following characteristics: frequency range, number of channels, power rating, transfer efficiency, isolation response, and impedance matching capability which is expressed in terms of an allowable antenna VSWR.

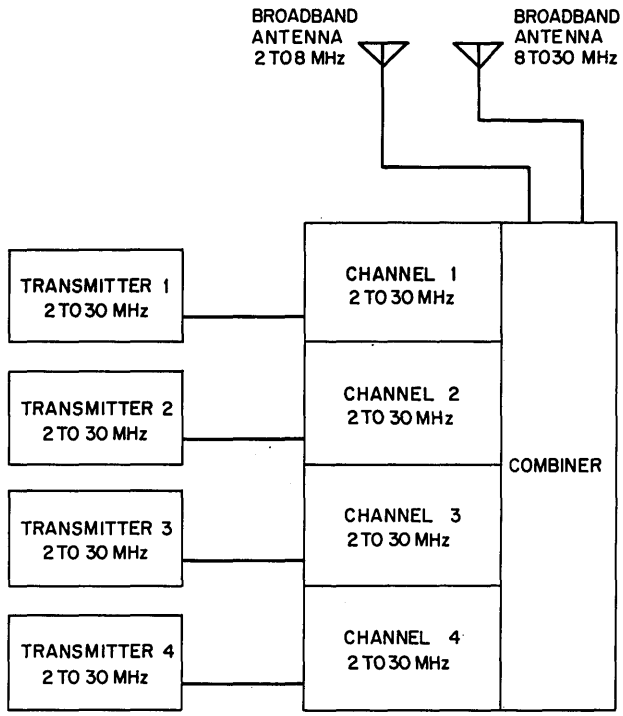

Fig. 4 — Improved small-ship distribution system (referred to hereafter as the self-contained selective distribution system (SSDS))

In adapting the technology of RF distribution systems to the constraints of ships having four or five transmitters, the following objectives for the SSDS have been established:

Frequency Range — Each channel has a 2 to 30 MHz range in two bands of 2 to 8 MHz and 8 to 30 MHz;

Number of Channels — A capacity of at least four channels and preferably five must be provided;

Power Rating — 1 kW average power, 2 kW peak envelope power per channel;

Transfer Efficiency — RF output to RF input, ratio, minimum 55 percent (2.6 dB);

Isolation Response — A minimum of 35 dB at 5 percent separation from the operating frequency;

Impedance Matching Capability — Operate into antennas with a VSWR as high as 4.0 over the entire frequency range.

The general approach employed in the SSDS is shown for one channel in the schematic diagram of Fig. 5. The tunable filter is formed from a set of coupled band-switched resonators. Two input coupling loops, each appropriate to a segment of the frequency range, are in proximity to each input resonator. Each of the two output coupling loops in proximity to the output resonator feed one of the two separate output combining networks. Channels to accommodate additional transmitters are represented in Fig. 5 by the lumped inductance elements which feed impedance compensation networks completing the RF path to each antenna.

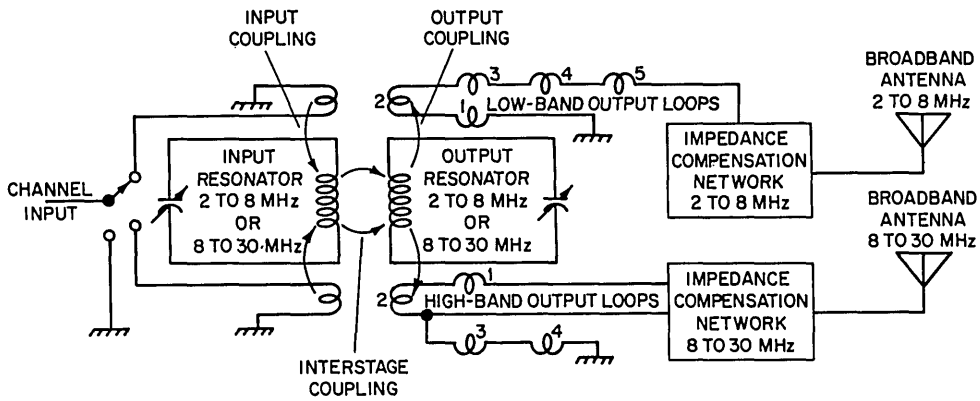

Fig. 5 — RF path for one channel of the SSDS

There are two key problem areas attendant to this approach: the development of a multiple-output combining network and the development of a 2-kW (PEP) wide-range (2 to 30 MHz) tunable filter.

Experimental Design

The filter portion of each channel consists of two resonators that are tuned to form a narrow frequency passband. Each resonator comprises an inductor and a variable vacuum capacitor. By controlling the degree to which each resonator is loaded, the passband and stopband responses are established. Energy is coupled into the input resonator from the transmitter by means of a single-turn loop. Magnetic interstage coupling transfers the energy to the output resonator. Likewise energy is transferred by means of a loop from the output resonator into the antenna via the combining network.

To accommodate a wide range of antenna impedance, the output coupling loops must be adjustable with respect to the output resonator inductor. The highest magnetic flux concentration occurs central to and coaxial with the resonator inductor. The design shown in Fig. 6 permits both of the output loops to be positioned for near-optimum coupling. The two output coupling loops are arranged inside the resonator inductor. The rotational axis for the loops are mutually perpendicular, allowing each output coupling loop to rotate through an arc of 90 degrees. This arrangement permits either loop to be

independently positioned from a minimum-coupled condition to maximum with respect to the resonator inductor. For the intended application one loop is always in a near-minimum-coupled position. Drive shafts and loop connections pass through bushings at 90-degree intervals around the center turn of the resonator inductor. Mechanical interference between loops is avoided by making the diameter of the high-band loop slightly smaller than the diameter of the low-band loop.

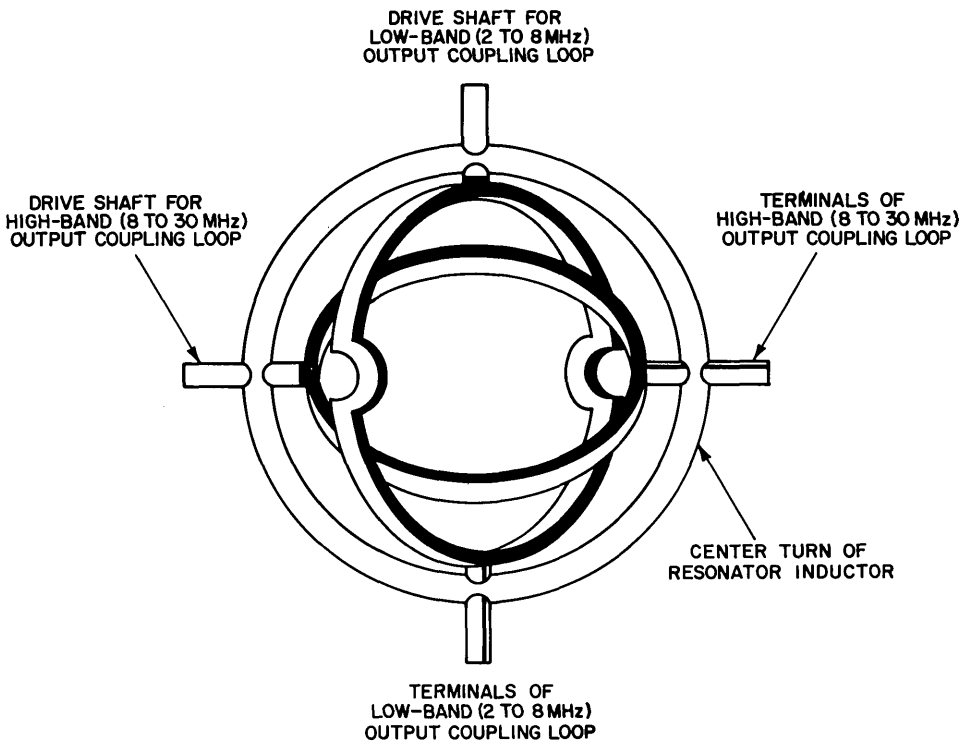

Fig. 6 — Arrangement of inductor and coupling loops permitting the loops to be independently rotated between positions of minimum and maximum coupling

Another problem area is the design of a resonator that can be tuned over the complete 2 to 30 MHz frequency range. Tuning over a 15 to 1 frequency range cannot be accomplished with techniques currently used without resorting to a switching technique to change the inductance of the resonator. Additional design constraints are established by the voltage and current, the Q factor, and the requirement that the size and shape of the resonator inductor yield an acceptable coefficient of coupling to the output loops. For thermal reasons the active conductor surface area of the resonator inductor should be approximately the same for either the high- or low-band configuration.

Various resonator inductors have been designed, constructed, and evaluated in terms of the inductance, Q factor, and maximum coefficient of coupling for the high- or low-band frequency range. The results of this effort culminated in a band-switched resonator design that is schematically shown in Fig. 7. The inductor portion of the resonator is made up

of three 2-turn coil sections. In the lower frequency band the three-coil sections are series connected. For the higher frequency band a switching mechanism reconfigures the coil windings for a parallel connection. A photograph of the resonator inductor and band-switching arrangement is shown in Fig. 8. The terminals of each two-turn coil section of the winding are brought to switch terminal blocks mounted on an insulator plate. Each block contains a ring of beryllium copper fingers machined from one piece of cylindrical tempered stock. The inner surface of each finger is contoured to uniformly contact a rod that completes the connection between switch blocks. Approximately 2 inches of movement is required of the rods to effect the band change. The entire winding is active in both switch positions, with no short-circuited or open-circuited turns. In Fig. 9 is shown the Q characteristics of an optimized band-switched-resonator assembly as a function of frequency. The parameters of various resonators built in evolving the design shown in Fig. 8 are presented in Appendix A.

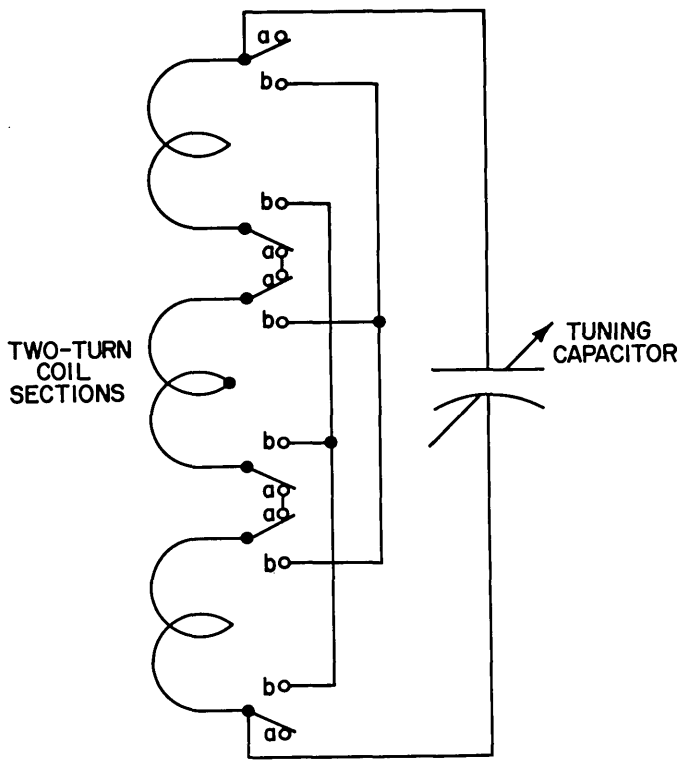

Fig. 7 — Resonator band-switching arrangement. In band-switch position "a" (as shown) the two-turn coil sections are series connected for low-band operation. In bandswitch position "b" the two-turn coil sections are parallel connected for high-band operation.

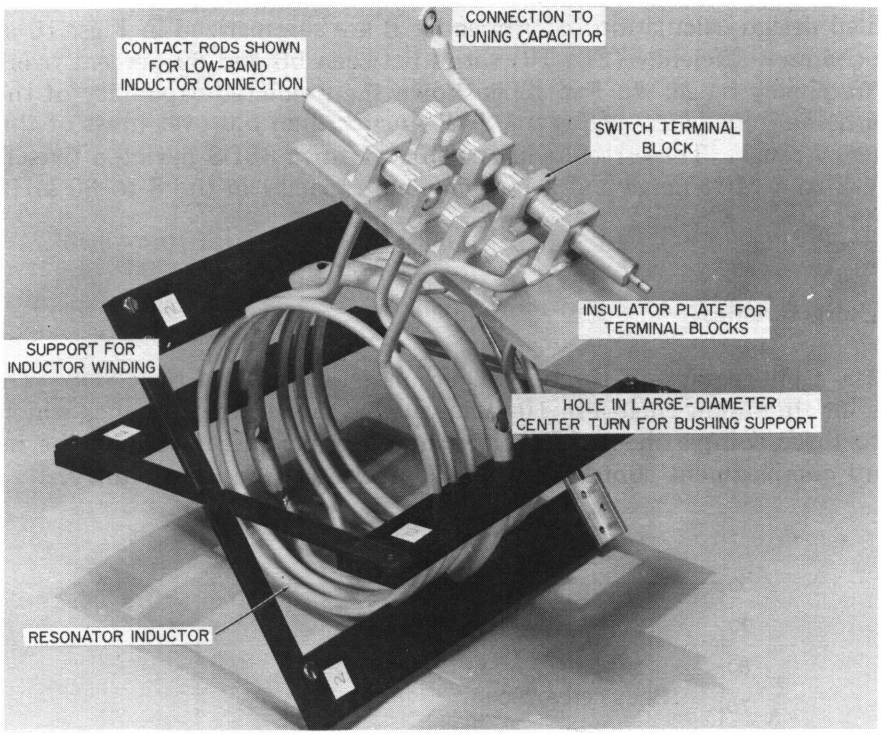

Fig. 8 — Band-switching assembly

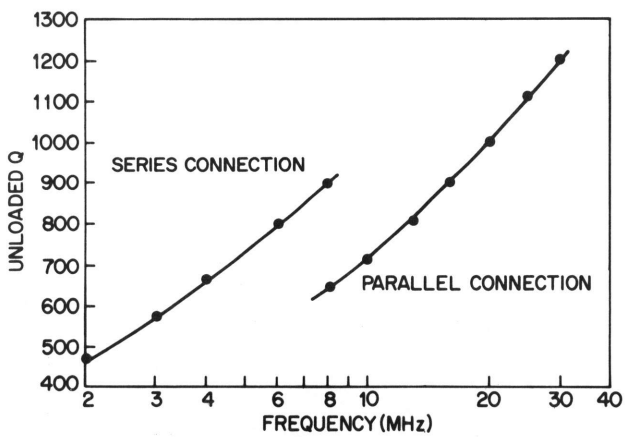

Fig. 9 — Resonator Q characteristics

Calculations have been performed to relate the basic parameters of the optimized resonator assembly with a compatible combining arrangement to produce the design values of resonator performance. Appendix B is a tabulation of the results of these calculations and provides detailed information on the combining arrangement. A series type of combining arrangement is used in the 2 to 8 MHz range in which five output coupling loops are series connected to the antenna and impedance compensation networks. For the 8 to 30 MHz band a combining arrangement similar to that used in the AN/SRA-58 multicoupler is employed. Combining is accomplished by the parallel connection of two groups of coupling loops to the antenna via an impedance compensation network. Each group consists of a series connection of two output coupling loops.

The detailed design calculations of Appendix B are summarized in Figs. 10 and 11. The predicted channel efficiency (Fig. 10) varies between 56 and 69 percent over the 2 to 30 MHz frequency range. In Fig. 11 is shown the predicted capability of the SSDS to match an antenna impedance having a VSWR greater than 5.0 over most of the 2 to 30 MHz frequency range. These results are calculated for a SSDS having a five-channel capacity in the 2 to 8 MHz range and a four-channel capacity in the 8 to 30 MHz range as shown in Fig. 12.

Performance Characteristics

Figure 13 is a photograph of the one experimental channel of the SSDS. The circuitry is contained in an aluminum enclosure 10 inches by 28 inches by 30 inches which is partitioned into three compartments. The two large compartments contain the resonators, and the forward compartment contains various control and monitor circuitry.

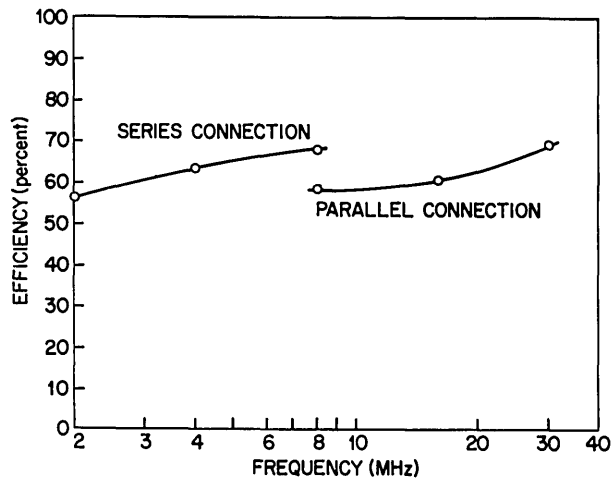

Fig. 10 — Predicted channel efficiency

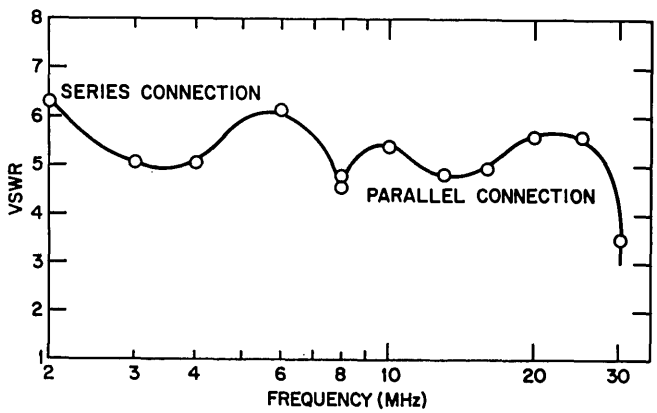

Fig. 11 — Predicted impedance-matching capability (VSWR)

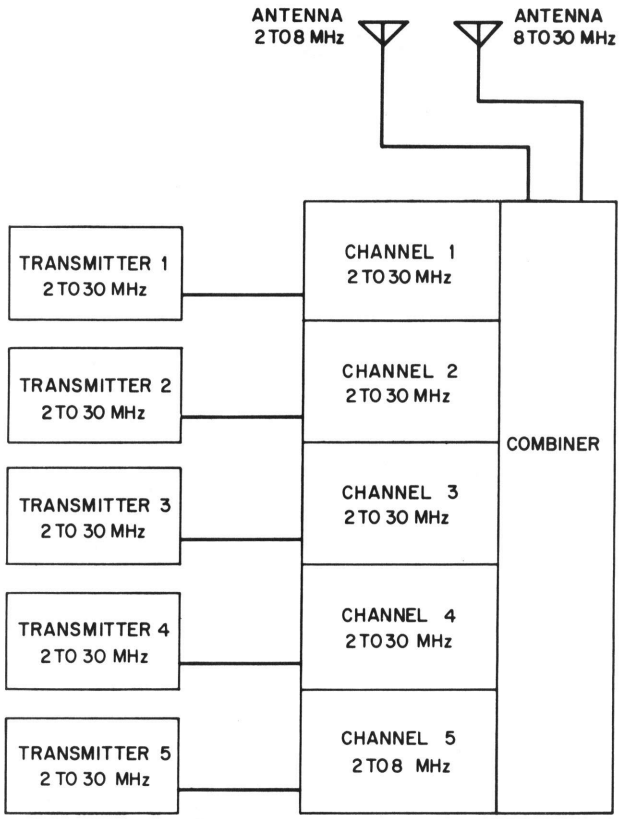

Fig. 12 — Projected full-scale version of the SSDS

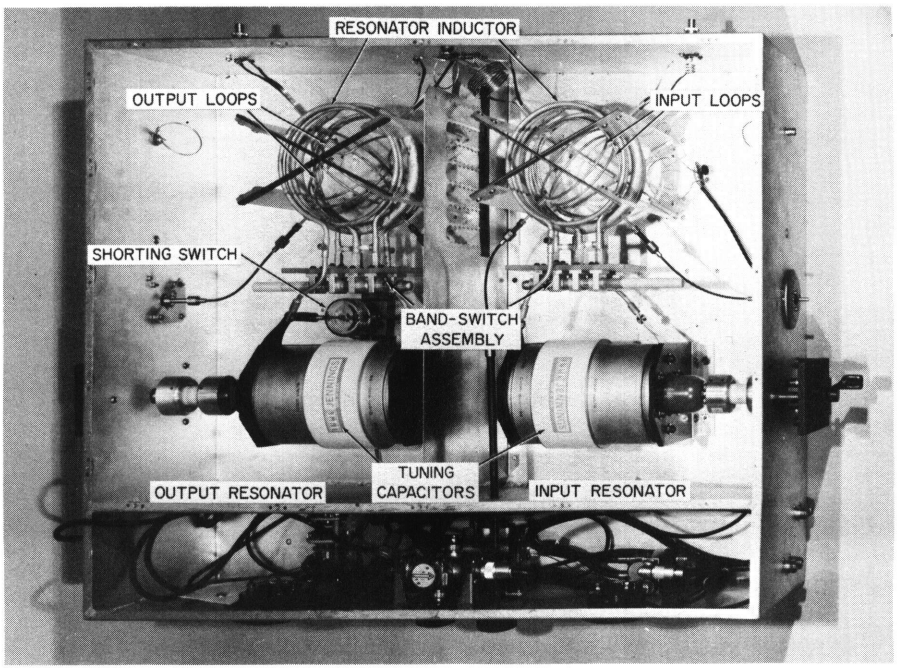

Fig. 13 — Experimental channel of the SSDS

Performance of the experimental channel was measured when it was operated into a mockup of the combining network as shown in Fig. 14. The values of the lumped-constant components used in the mockup combining network were selected from those readily available and therefore did not in all cases exactly duplicate the design values shown in Appendix B. The mockup combining network simulates the additional channels that would be present in a full-scale version of the SSDS.

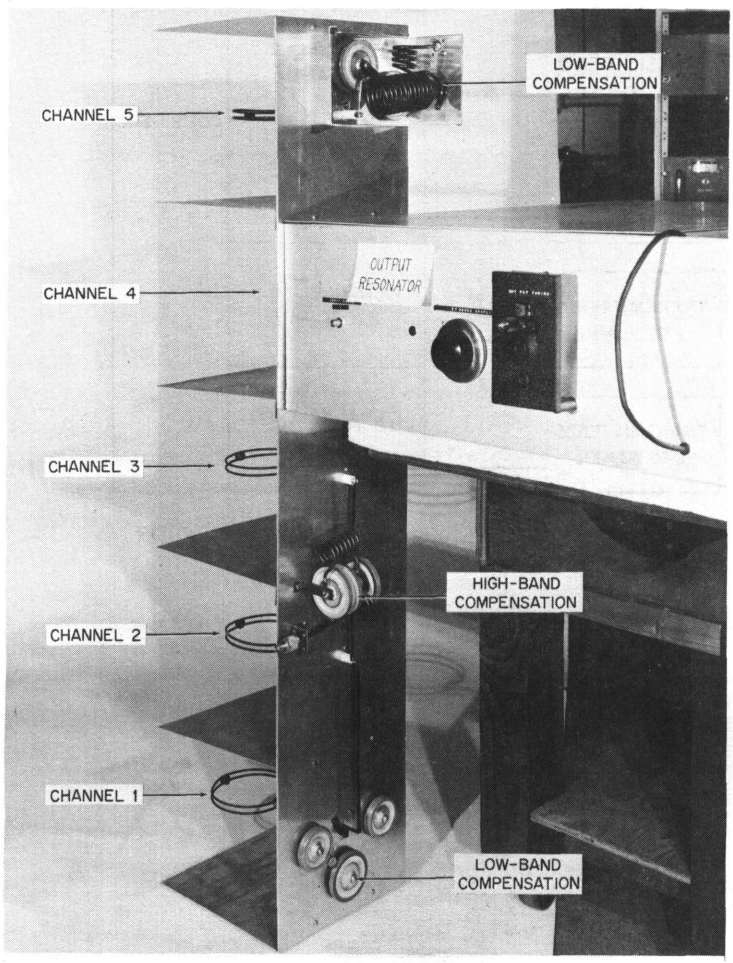

Fig. 14 — Mockup of the output distribution networks of the SSDS with the experimental channel

Figure 15 shows that the measured transfer efficiency of the experimental channel as a function of frequency to be between 55 and 71 percent. This efficiency corresponds to insertion-loss values between 2.6 and 1.50 dB.

Figures 16a through 16f show forward selectivity response characteristics between 0.1 and 35 MHz for the experimental channel when it is tuned to various frequencies between 2.0 and 30.0 MHz. These data show the response to be down 35 dB or more at frequencies greater or less than 5 percent of the operating frequency. Figure 17 is a plot of the 3-dB bandwidth as a function of operating frequency. The narrowest bandwidth of 20 kHz occurs at 2.0 MHz and increases to 195 kHz at 30 MHz.

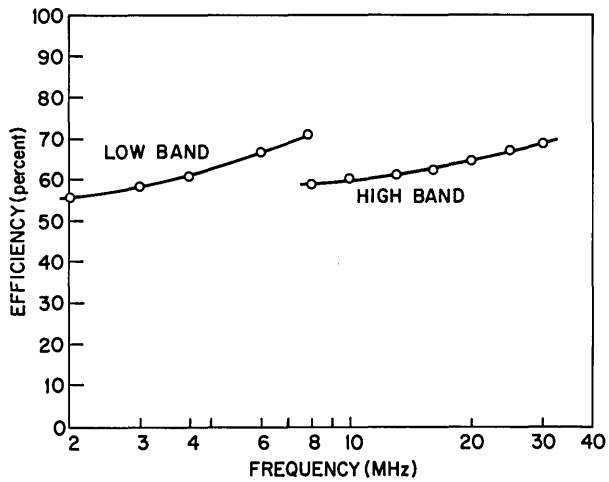

Fig. 15 — Measured transfer efficiency of the experimental channel

The impedance-matching capability of the experimental channel has been determined at three frequencies in both the 2 to 8 MHz and 8 to 30 MHz bands. The procedure consisted of operating the channel into various termination impedances that collectively described impedance loci of constant VSWR. The terminations were constructed from resistively terminated sections of 50-ohm transmission line. The effective transmission line length was varied in steps of 0.05 wavelength at each frequency. For each termination the output resonator tuning and coupling controls were adjusted to provide a minimum VSWR as measured at the input terminal of the experimental channel. Figure 18 shows the termination VSWR for which a matched condition (VSWR $\leqslant$ 1.05) at the channel input can be achieved. In the low band (2 to 8 MHz) the VSWR matching capability was determined to be at least 5.0 at 2.0 and 4.0 MHz and 4.0 at 8.0 MHz. In the high band (8 to 30 MHz) the VSWR matching capability is 3.4 at 8.0 MHz and becomes 5.0 or greater from approximately 16 to 30 MHz. The biggest discrepancy between the predicted and actual VSWR matching capability values occurs in the 8 to 30 MHz band. Improvement over the performance of Fig. 18 is considered achievable by additional optimization of the impedance-compensation networks.

Maximum resonator voltages are developed in the low band at 8 MHz and in the high band at 30 MHz (Appendix B). Although the maximum voltages in each band are approximately the same (about 13 kV), the voltage gradients in the resonator are about three times larger at 30 MHz than at 8 MHz (low band). Accordingly, to prove the ability of the experimental channel to withstand the highest of the voltage stresses, short-term power-handling tests have been applied at 30 MHz. The results of these tests confirm a single-channel power-handling capability equivalent to 2700 watts PEP at 30 MHz. In addition short-term power tests have been applied at 2, 4, and 8 MHz in the low band and 8 and 16 MHz in the high band at power inputs in excess of 2000 watts PEP. Sustained power-handling tests will be made upon completion of the construction of the direct evaporative cooling system which will circulate refrigerant through each resonator winding (Fig. 19).

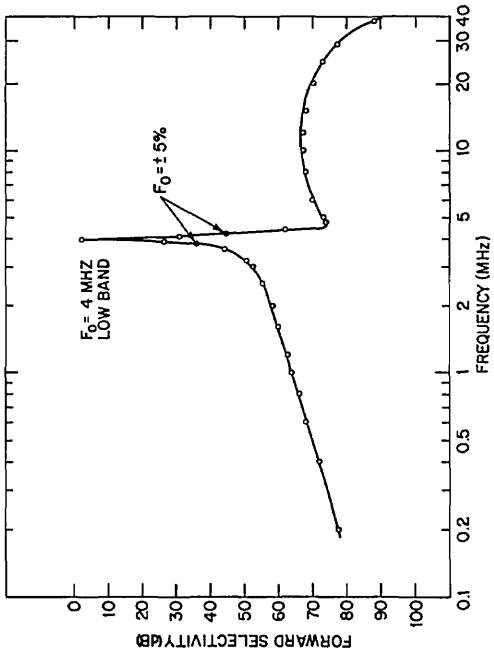

Fig. 16b — Response characteristics of experimental channel when tuned to 4.0 MHz (low band)

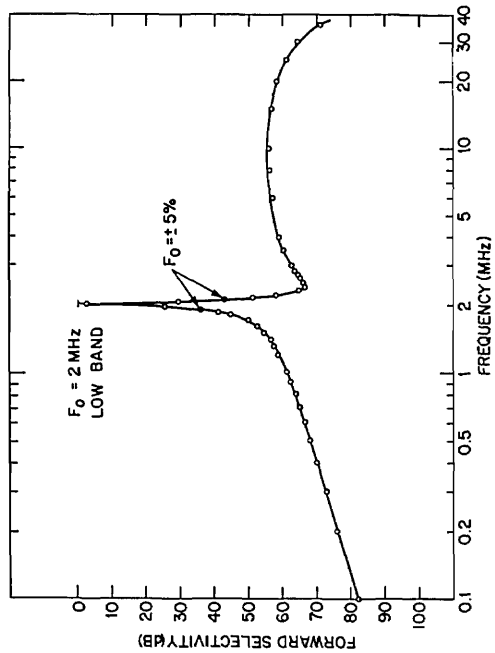

Fig. 16a — Response characteristics of experimental channel when tuned to 2.0 MHz (low band)

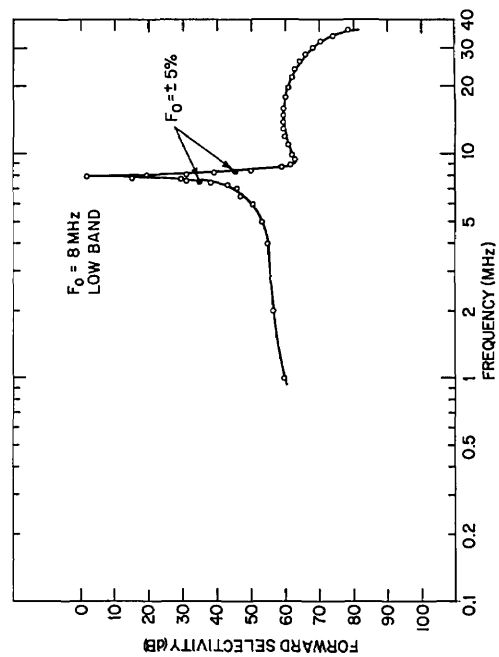

Fig. 16c — Response characteristics of experimental channel when tuned to 8.0 MHz (low band)

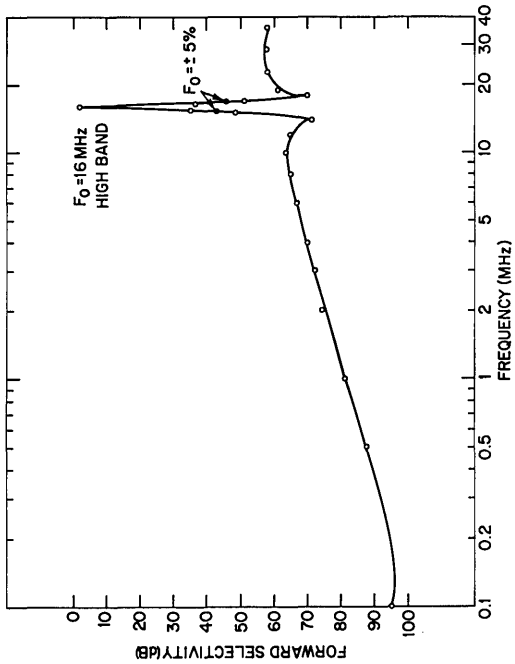

Fig. 16e — Response characteristics of experimental channel when tuned to 16.0 MHz (high band)

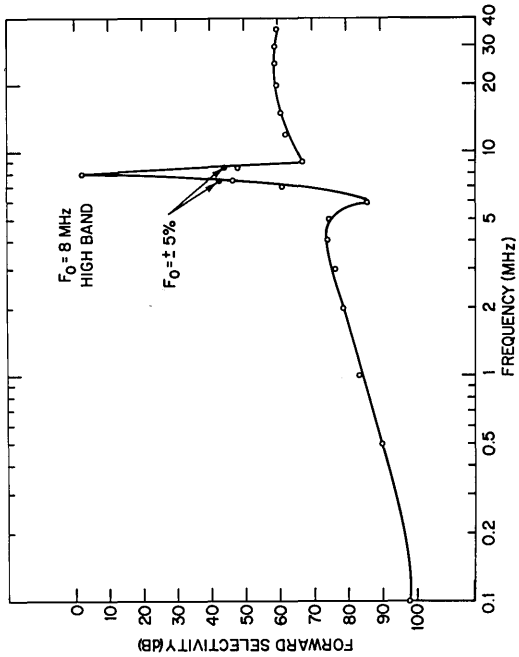

Fig. 16d — Response characteristics of experimental channel when tuned to 8.0 MHz (high band)

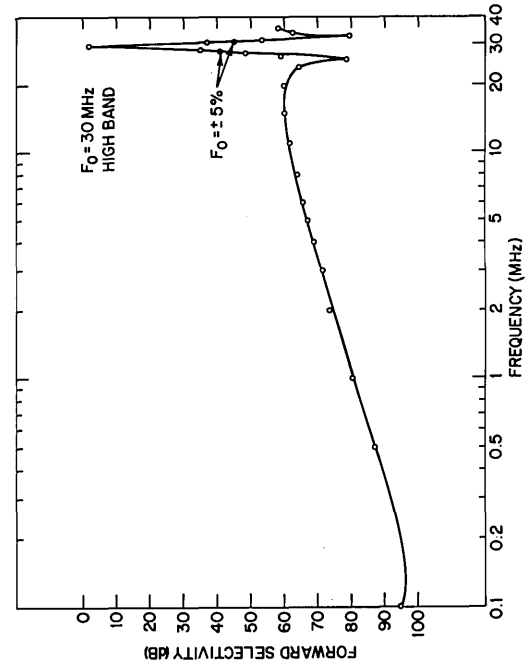

Fig. 16f — Response characteristics of experimental channel when tuned to 30.0 MHz (high band)

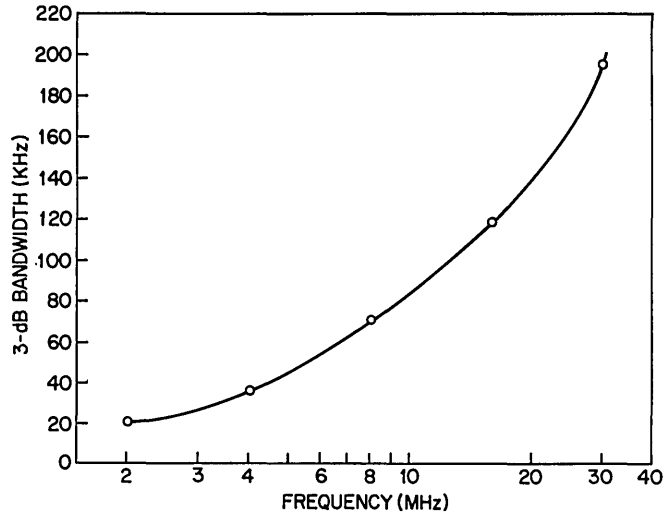

Fig. 17 — Three dB bandwidth of experimental channel as a function of operating frequency

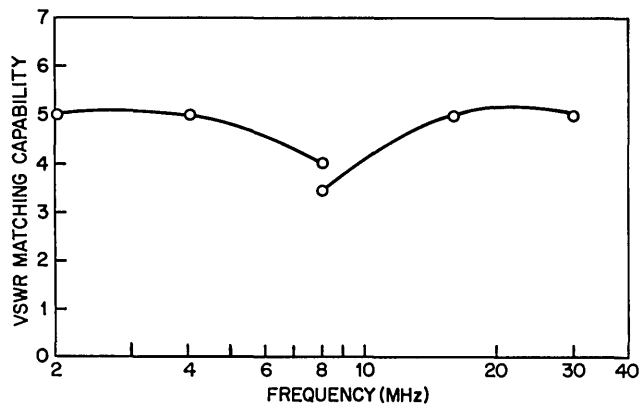

Fig. 18 — Impedance matching capability (VSWR relative to 50 ohms) of the experimental channel

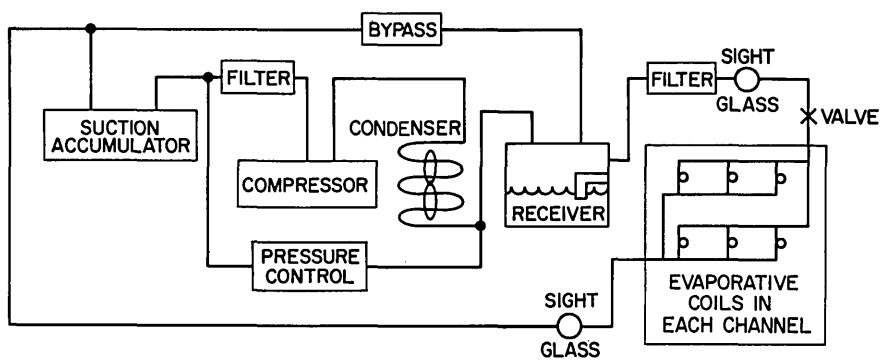

Fig. 19 — Direct evaporation cooling system for the SSDS

SYSTEM CONSIDERATIONS

Based on the performance of the experimental channel the feasibility of the SSDS concept is established. Many details need to be resolved in the succeeding phases of SSDS development before an operational design is achieved. Some of these details are of a systems nature.

Automation

To fulfill the potential performance of which the SSDS is capable, an automatically tuned version needs to be developed. An automated equipment would require the adaption of motorized drive mechanisms for all variable elements and the necessary control, alarm, and remote status indication circuitry. Figure 20 is a diagram illustrating automation aspects of the SSDS.

Figure 20 shows the switches in an alert or home position. Assuming normal operation, when a transmitter is keyed, the RF energy is applied to the attenuator portion of the SSDS channel. The attenuator provides a 50-ohm termination which enables proper tuning of the transmitter and allows energy at a reduced level to be delivered to a logic circuit and the input loop (L_3) via the impedance sensor and selector switch (SW_3) respectively.

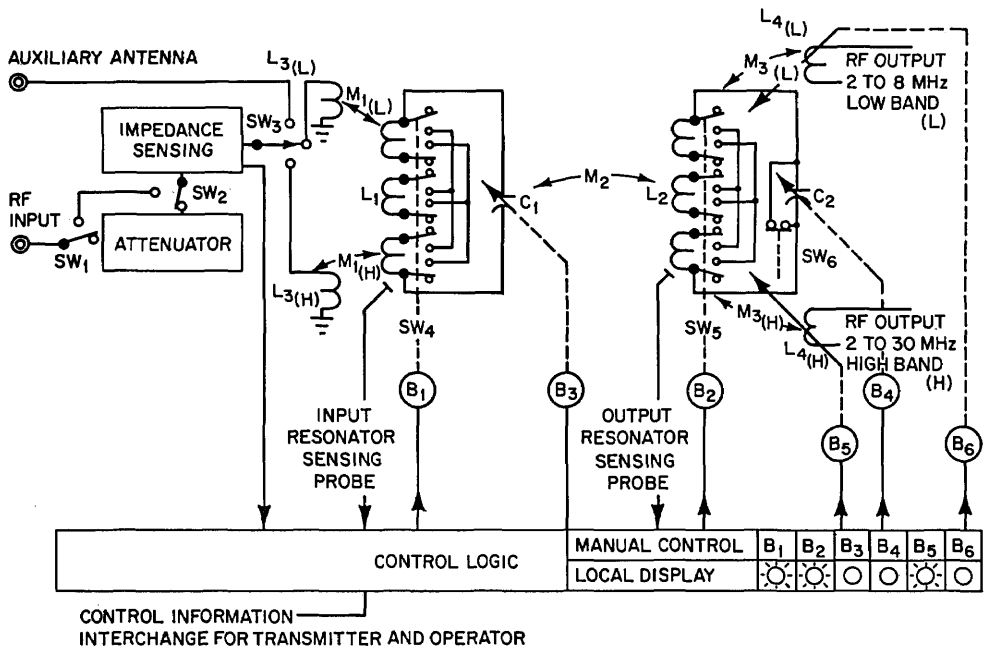

Fig. 20 — Automation and control aspects of the SSDS

The attenuated signal is fed to the control logic circuitry, which determines if the frequency is in the low band (2 to 8 MHz) or in the high band (8 to 30 MHz). Motors B_1 and B_2 are activated to change the switch assemblies SW_4 and SW_5 if the frequency is determined to be in the high band; however, if the frequency is in the low band, B_1 and B_2 are not activated and SW_4 and SW_5 remain in the low-band position. The contacts of SW_3 remain positioned for the low-band input loop unless information is fed from the control logic circuit to change to the high-band input loop. The control logic circuit will designate one output loop to be activated and the other decoupled by information fed to B_5 and B_6.

After the control logic has selected the proper components and switch contacts, the reduced-level signal is fed to the input resonator via SW_1, the attenuator, SW_2, the impedance sensing network, and SW_3. The input resonator capacitor (C_1) is tuned by motor B_3 as initiated by the control logic. Resonance is determined by the control logic circuit from a signal fed back via the input resonator sensing probe. When the input tuning is accomplished, SW_6 takes the short off the output resonator. Motors B_4 and B_5 or B_6 are activated to tune and load the output resonator for 50 ohms at the channel input. Having completed tuning, the control logic circuit sends dekeying information to the transmitter. Then the SW_1 and SW_2 contacts are transferred to the operate position, thus bypassing the attenuator. The channel is now ready to transfer rated power to the antenna. The equipment remains in the operate mode until commanded to return to the alert or home mode.

The projected SSDS design will include a semiautomatic backup capability with local control of the necessary functions for operation. A feature under consideration is a separate detachable panel that includes the local control and display, making it possible to remotely locate this panel at say 100 or 200 feet from the SSDS.

Provision for Auxiliary Antenna

It will be necessary or desirable occasionally to bypass the SSDS and operate into other existing antennas. A switch arrangement, Fig. 20, shows a bypass path from the channel input via SW_1, SW_2, and SW_3 to an auxiliary output terminal.

Installation

An automated SSDS will provide for all necessary internal switching between the transmitters and the antennas. Therefore the amount of RF and control cabling required in an SSDS installation will be substantially less than that required for a current installation. Furthermore, the SSDS could be installed in a remote space relieving congestion in the radio-room.

Based on the size comparison shown in Fig. 21 the SSDS achieves a volume reduction of approximately 60 and 40 percent when compared to current manual and automatically tuned distribution systems.

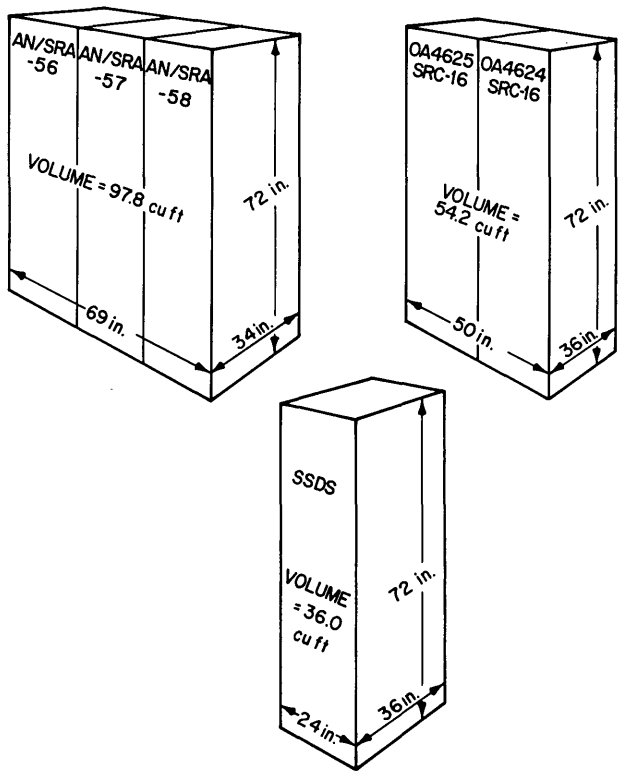

Fig. 21 — Size comparison of the SSDS to existing Navy distribution systems

Antenna Requirements

The SSDS requires two broadband antennas with a VSWR not exceeding 4.0: one designed for the 2 to 8 MHz range and one for the 8 to 30 MHz range. Designs for broadband antennas compatible with the SSDS for specific classes of ships are being investigated by the cognizant Navy activities. No insurmountable design problems are anticipated.

Companion Receiving System

A receive distribution system using the most recently developed AN/SRA-49 shipboard receive multicoupler, as shown in Fig. 22, provides 20 receiving channels from one antenna. Six channels each cover the 2 to 6 MHz and 4 to 12 MHz frequency ranges, and four channels each cover the 10 to 17 MHz and 17 to 30 MHz frequency ranges. A patch panel is provided to permit the associated receivers to be connected to an appropriate channel. Each channel, when tuned (manually), provides an extremely narrow passband centered on the operating frequency and permits a receive channel to be tuned to within 3 percent of the frequency of a local transmitter before excessive interference occurs.

The AN/SRA-49 receive multicoupler provides excellent performance, but other approaches may be capable of providing equivalent electrical performance with greater flexibility, requiring less operator attention, and the equipment would occupy less space. One possibility is illustrated in Fig. 23 and consists of the antenna, an input distribution network,

and an active multicoupler. The multicoupler provides up to eight broadband outputs, each of which can be dedicated to a 2 to 30 MHz receiver. Additional outputs could be provided by a cascade connection of a second multicoupler to one of the outputs. The active multicoupler must be capable of extreme linearity, have a low noise figure, and have moderate gain characteristics. Current state-of-the-art active multicouplers are believed to be capable of meeting the requirements subject to a correct systems design of the antenna and input distribution network. The input distribution network would include a group of notch filters to suppress the amplitude of coupled energy from local transmitters and effectively extend the dynamic range of the multicoupler. The tuning of the notch filters must correspond to the frequency of the local transmitters. Accordingly the control of the notch filters should be managed by the transmit portion of the distribution system. The SSDS could readily be designed to accommodate the necessary control functions of the notch filters used in the input distribution network.

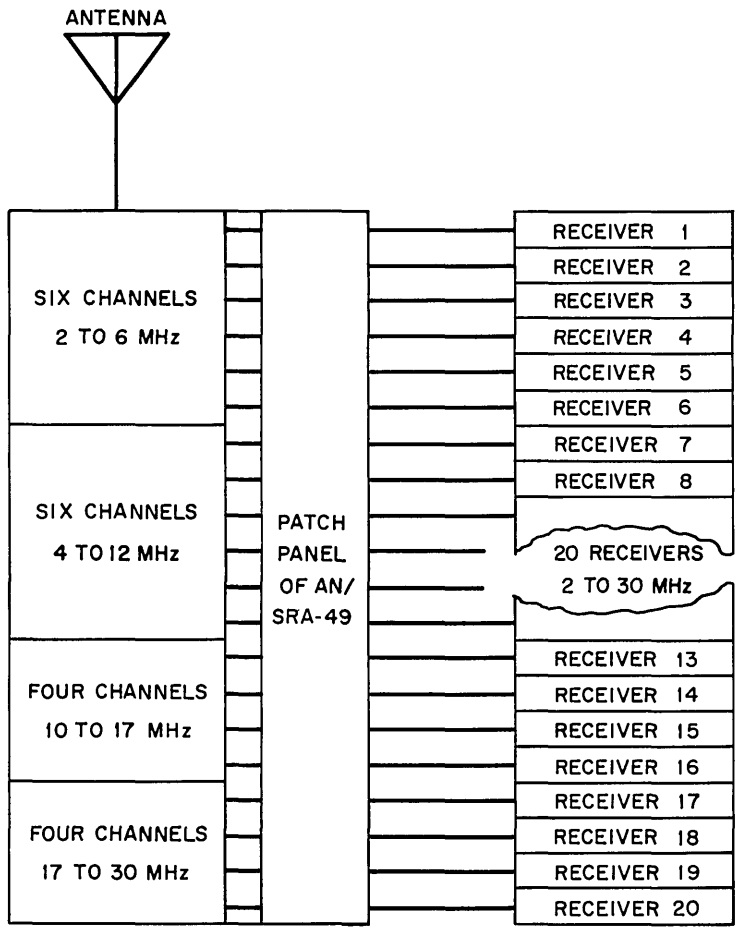

Fig. 22 — AN/SRA-49 conventional receive distribution system

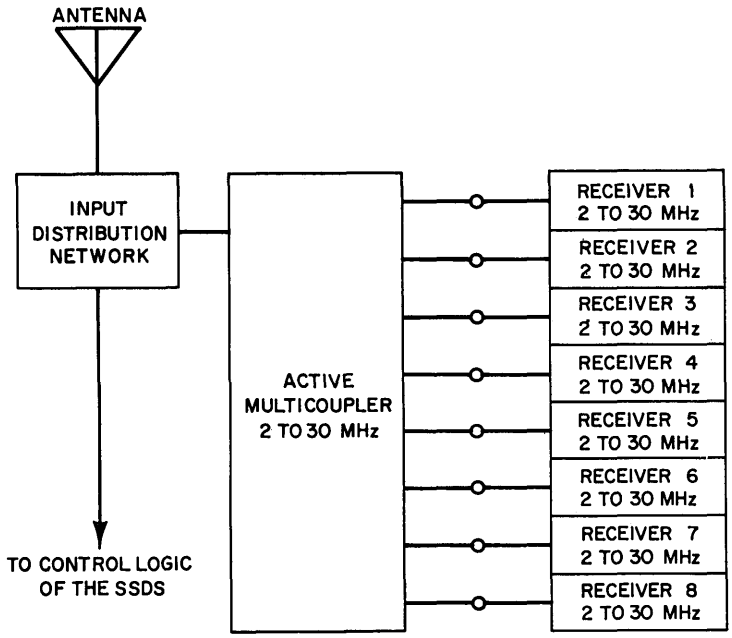

Fig. 23 — Proposed companion receive system for use with the SSDS

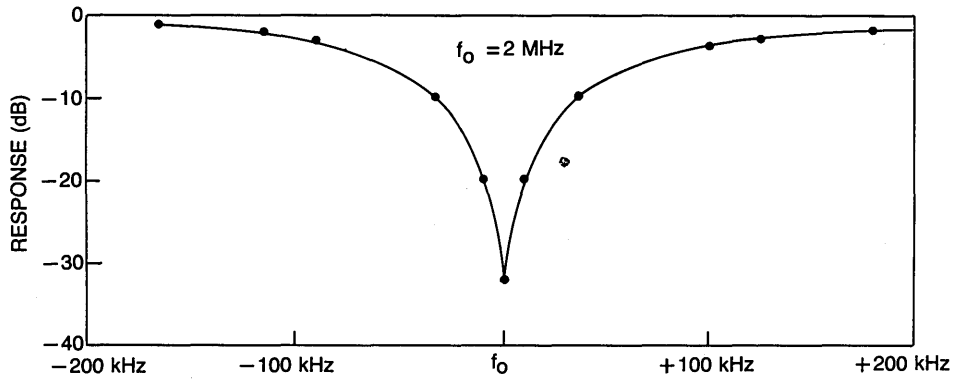

Fig. 24 — Response characteristics of an experimental notch filter

Tuneup of the appropriate notch filter would be simply one additional step in the tuneup procedure of a transmit channel. Figure 24 shows the response characteristics of an experimental tunable notch filter designed at NRL that has possible application.

There are at least two advantages in using this approach:

- The RF distribution path for both transmission and reception is established and controlled by a single system.
- The receive system operator is relieved of any tuning and patching duties. He can operate his receiver in a scan mode, if desired, and can change frequency much more rapidly.

CONCLUSIONS

An analysis shows existing RF distribution systems to be inadequate for ships having no more than four or five transmitters.

A customized RF distribution system must be designed for those ships having four or five transmitters or less. The design objectives have been established to satisfy the requirements for such a system.

The proposed SSDS transmit design satisfies the objectives and requirements for the ship with less than five transmitters. The SSDS design will eliminate the need for switching and patching panels. The equipment can be located in a remote area away from the radio spaces, it will occupy considerably less space, and it will require fewer antennas. A complete single channel with four simulated channels, built and tested, has verified that the SSDS design will meet the requirements.

The adaption of a direct evaporative cooling technique to the SSDS has proven to be an important advancement in removing heat at the point of generation and thereby improving the thermal stability.

A companion receive distribution system has been proposed for use with the SSDS. The technique would provide central management and control of both the receive and transmit distribution functions.

RECOMMENDATIONS

An advanced development program should be initiated and supported to develop and construct a model of the SSDS. This model should be automatically controlled and have the capability to accommodate five transmitters.

An exploratory development program should be initiated and supported to develop the SSDS so that one of the five transmit channels would have the capability to handle 5 kW PEP. The system would then satisfy the NTDS requirements.

The proposed companion receive distribution system should be initiated and supported as an exploratory development program.

ACKNOWLEDGMENT

The authors wish to thank Mr. M.L. Musselman and Mr. W.D. Long of the Naval Research Laboratory and Mr. R.W. Pride of the Naval Ship Engineering Center for helpful suggestions in the organization of this report.

Appendix A

EVOLUTION OF THE RESONATOR INDUCTOR

The approach to the SSDS resonator design was greatly influenced by goals originally set forth, which include: an operating range from 2 to 30 MHz and a multiple-output network capable of feeding at least two but not more than three antennas. The original intent was to design a system for ships having four or five transmitters.

A tentative resonator capacitor-inductor combination was initially selected from which performance values were computed. From these calculated goals for Q factor, inductance, capacitor range, magnitudes of voltage, and current, the physical size was established. The approaches leading to the design of an inductor having the desired Q and inductance are summarized in this appendix. The size of the enclosure used to contain the resonator inductor for Q measurements was approximately 10 by 15 by 22 inches.

The Q measurements in Fig. A1 are for a bifilar arrangement of two inductors. The unloaded Q was acceptable, but the inductance change between the series and parallel connections was not suitable for the selected capacitor to tune over the entire 2 to 30 MHz frequency range. A trifilar approach was considered as a method to accomplish the needed change in inductance; however the switching arrangement was too complex.

To conserve space an inductor and capacitor were arranged coaxially. When compared to a conventional arrangement, the Q was degraded by 30 percent (Fig. A2).

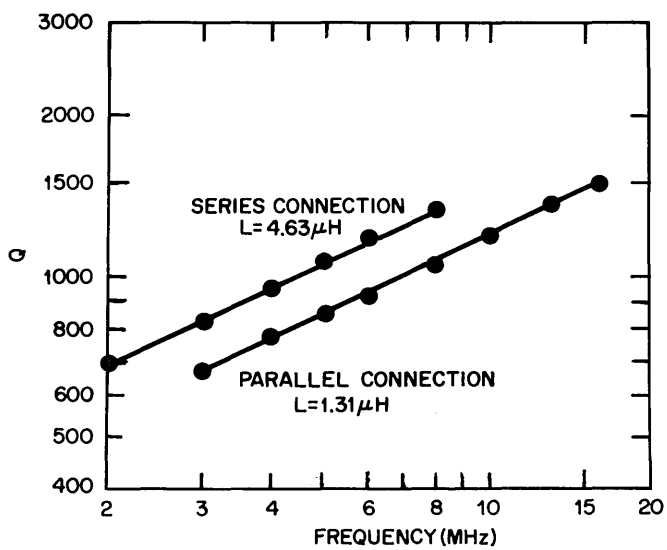

Fig. A1 — Q measurements for series and parallel connections of a bifilar-wound inductor. Each of the two sections consists of 4 turns of 3/8-inch copper tubing with pitch of 3/4 inch on a diameter of 6-1/2 inches.

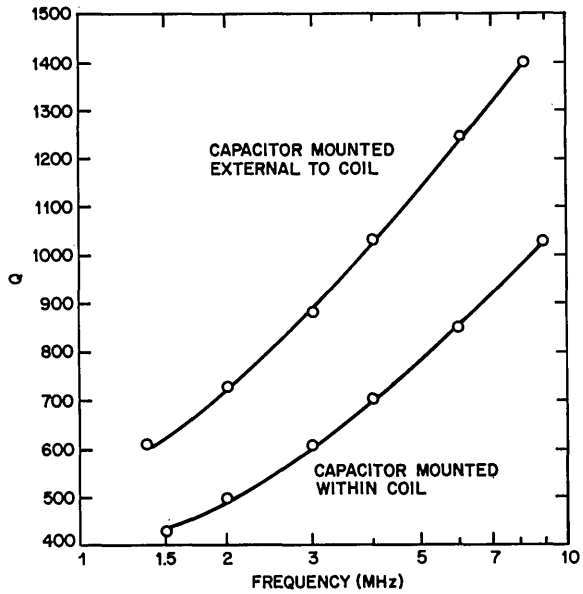

Fig. A2 — Measurements showing the degraded Q performance when the capacitor is mounted within the coil. The coil consists of 7-1/2 turns of 3/8-inch tubing with a pitch of 3/4 inch on a diameter of 5-7/8 inches.

Q measurements are shown in Fig. A3 for three arrangements of an 8 turn coil. The Q measurements for the coil when configured for the 2 to 8 MHz range were acceptable. In the 8 to 30 MHz range the unused portion of the 8-turn coil was either open or shorted, and the performance was unacceptable because of improper inductance or deteriorated Q.

Measurements of Q plotted in Fig. A4 were taken for three coils in a conventional arrangement to determine the maximum Q that could be expected from an ideal coil with the proper inductance.

In an effort to make the inductance range of the bifilar approach of Fig. A1 acceptable, a contrawound turn was added. The data of Fig. A5 shows that the Q measurements at the low end of the frequency range were deteriorated to the extent that the bifilar design was considered unacceptable.

The center turn of the inductor was designed to provide mechanical bearing surfaces for the loops to be associated with the resonator. Figure A6 shows Q measurements of a split bifilar arrangement having a common center turn and a half-turn contrawound on each side of the center turn. This design was dropped because the requirements for switching became overly complex.

Figure A7 shows Q measurements of three arrangements of an 8-turn coil. In the 2 to 8 MHz range the winding consists of a series connection of the 8 turns and provides acceptable Q performance but has excessive inductance.

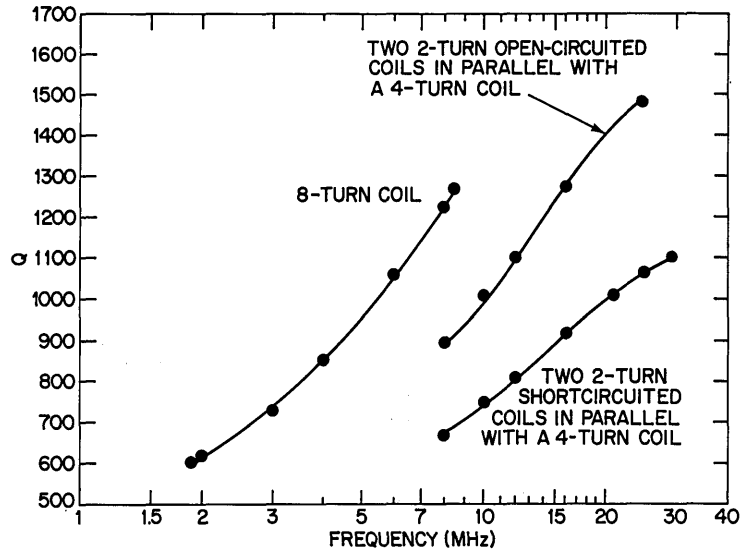

Fig. A3 — Effect of short-circuited and open-circuited turns on Q performance of an 8-turn coil consisting of 1/2-inch tubing with a pitch of 1 inch on a diameter of 5-3/4 inches. Inductance achieved for the open-circuited case did not permit operation to 30 MHz.

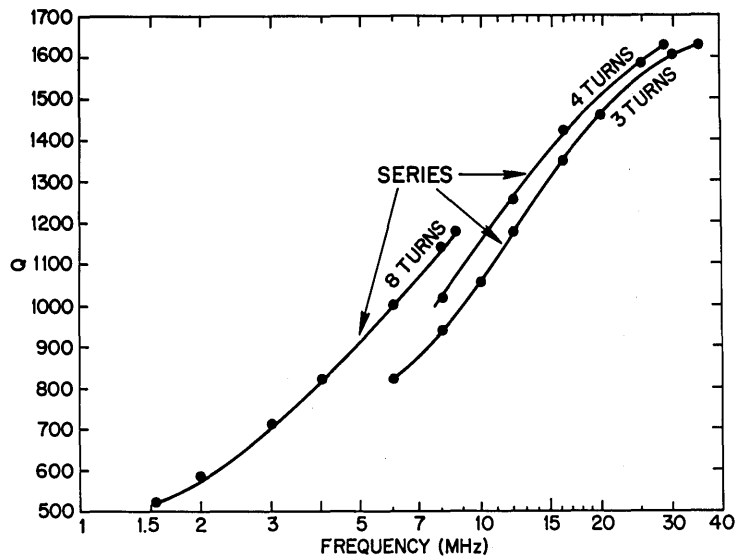

Fig. A4 — Q performance of conventional solenoid type inductors having the approximate inductance desired for each tuning range and built without regard to band-switching requirements. The coil consists of 1/2-inch tubing with a pitch of 1 inch on a diameter of 5-3/4 inches.

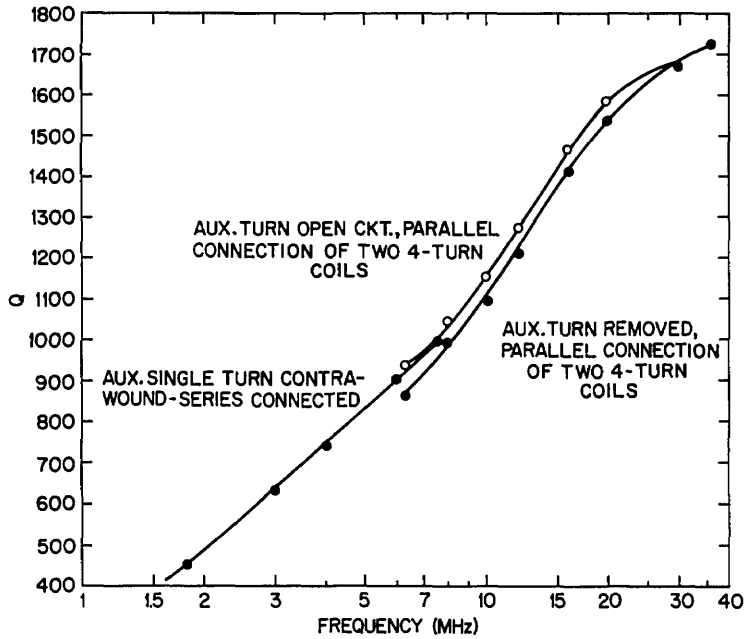

Fig. A5 — Effect of an auxiliary contrawound turn on Q performance of the bifilar inductor of Fig. A1

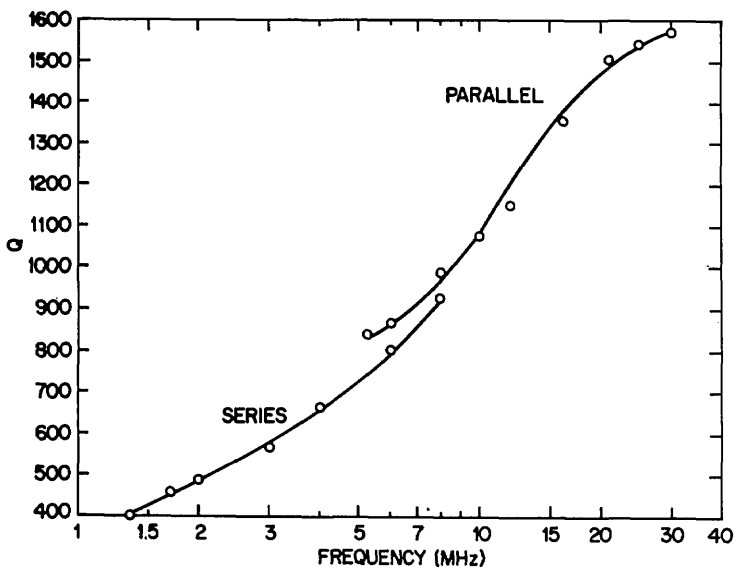

Fig. A6 — Q performance of a split bifilar winding with two contrawound half turns in the series connection. The contrawound half turns are left open-circuited in the parallel connection. There are 1-1/2 turns of 3/8 inch tubing, bifilar wound on each side of a center turn of 1/2 inch tubing all with a 3/4 inch pitch on a diameter of 6 inches.

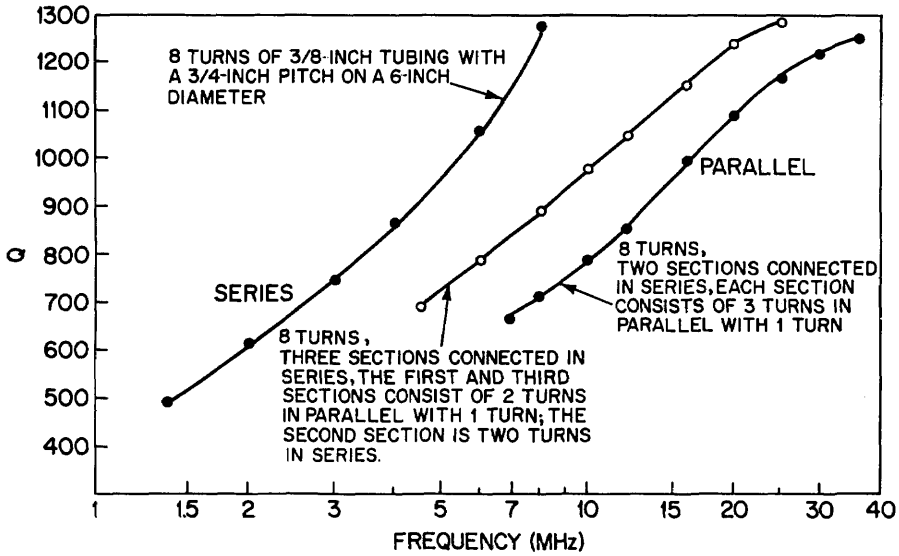

Fig. A7 — Q performance of an 8-turn inductor for various methods of connection

Each half of the winding when connected for the 8 to 30 MHz range includes an arrangement either of 1 turn in parallel with 2 turns and in series with 1 turn or of 1 turn in parallel with 3 turns. Both of the 8 to 30 MHz arrangements provided unacceptable Q performance. To reduce the inductance of the 8-turn winding of Fig. A7, a 6-turn winding was considered, with the results shown in Fig. A8. The Q performance is unacceptable in the 8 to 30 MHz range, and the inductance is insufficient in the 2 to 8 MHz range.

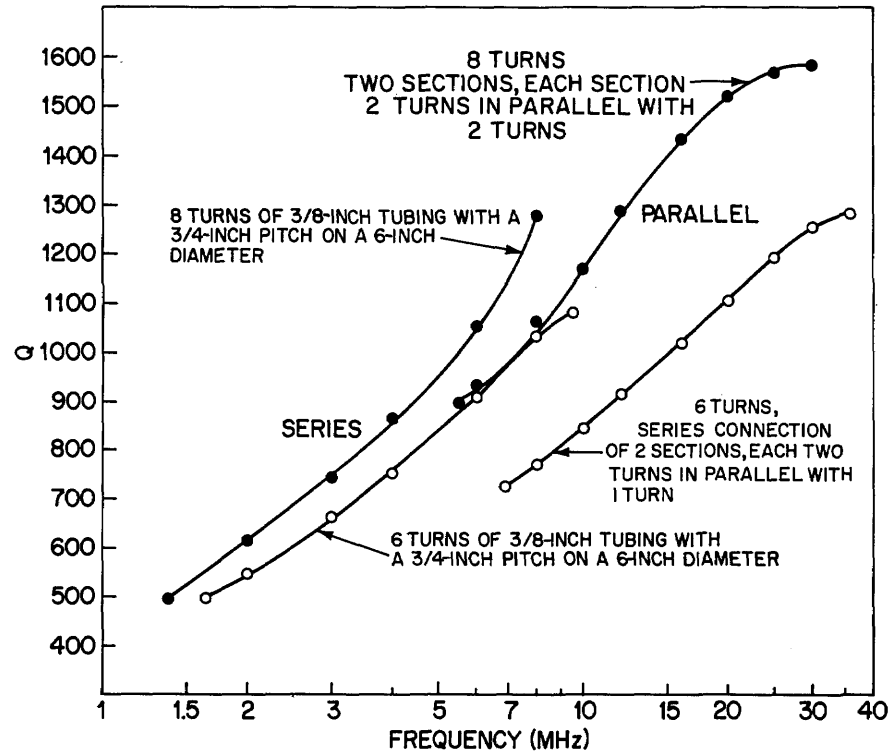

Fig. A8 — Q performance of 6- and 8-turn inductors for various methods of connection

Also shown in Fig. A8 are the Q measurements in the 8 to 30 MHz range for an 8-turn coil in which each half of the winding consists of two 2-turn windings in parallel. Observe that the inductance is excessive, but the Q measured is acceptable. The 6-turn coil has an arrangement of one turn in parallel with two turns on each side of the center, and has unacceptable Q performance.

Figure A9 shows Q measurements of a coil consisting of three 2-turn sections having acceptable Q and inductance. A series-connected (low-frequency) arrangement of this inductor is shown in Fig. A10. Figure A11 shows Q measurements for the same configuration with the 1/2 turn immediately adjacent to each side of the center turn reduced from 1/2-inch tubing to 1/4-inch tubing. This shortens the length of the coil and improves the coupling coefficient to the coupling loop. The design for the higher frequency band (three 2-turn coils in parallel) is shown in Fig. A12.

Having designed an acceptable inductor for the lower frequency band (2 to 8 MHz) and higher frequency band (8 to 30 MHz), consideration was given to the design of an appropriate switching mechanism. Figure A13 shows the first design of a switched inductor arrangement, permitting the sections of winding to be reconfigured from a series connection into a parallel connection. Figure A14 shows a comparison of Q measurements of the initial band-switched coil design and data of Fig. A11. The Q in the high band of the band-switched coil is greatly deteriorated and is unacceptable. Figure A15 is a second design of a switched coil having an improved lead arrangement. Figure A16 shows a comparison of Q measurements of the first design of the band-switched coil and the improved design. Figure A17 shows the Q measurements for the improved band-switched resonator when the coupling loops are installed. For these measurements the coupling loop appropriate for the particular band (2 to 8 or 8 to 30 MHz) was maximally coupled while the other loop was at minimum coupling. Both loops were open-circuited.

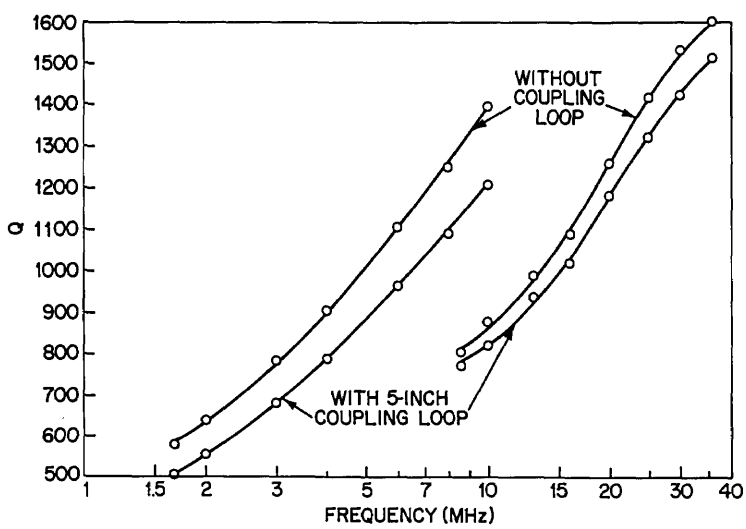

Fig. A9 — Q performance of series and parallel connections of a three-section, 2-turn-per-section, 6-turn inductor consisting of 2 turns of 1/2-inch tubing with a 1-inch pitch for the mid-section and 2 turns of 1/4-inch tubing with a 1/2-inch pitch for the other two sections, all on a 6-inch diameter

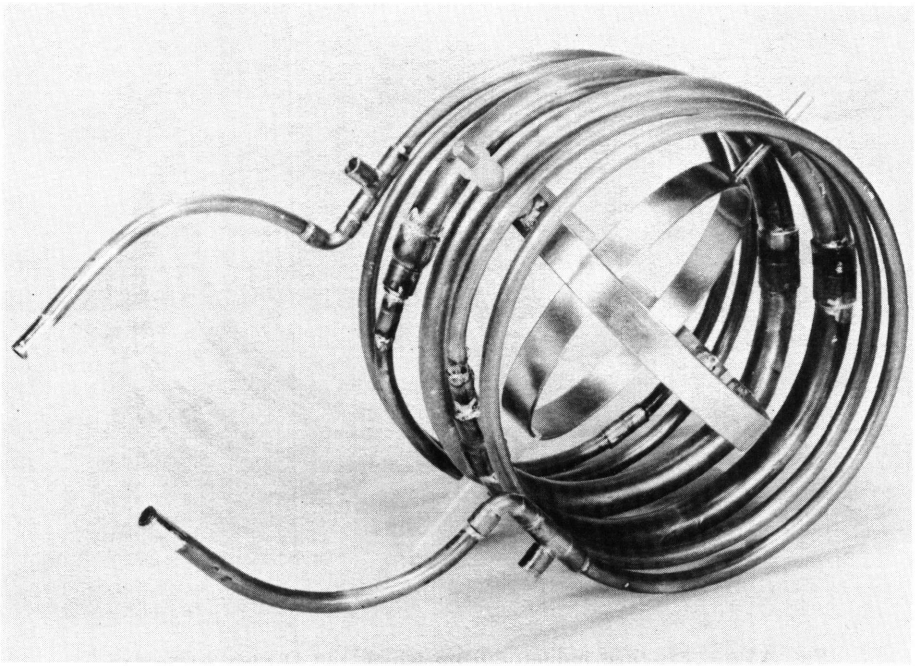

Fig. A10 — Six-turn inductor with coupling loops from which the Q measurements of Fig. A9 were obtained

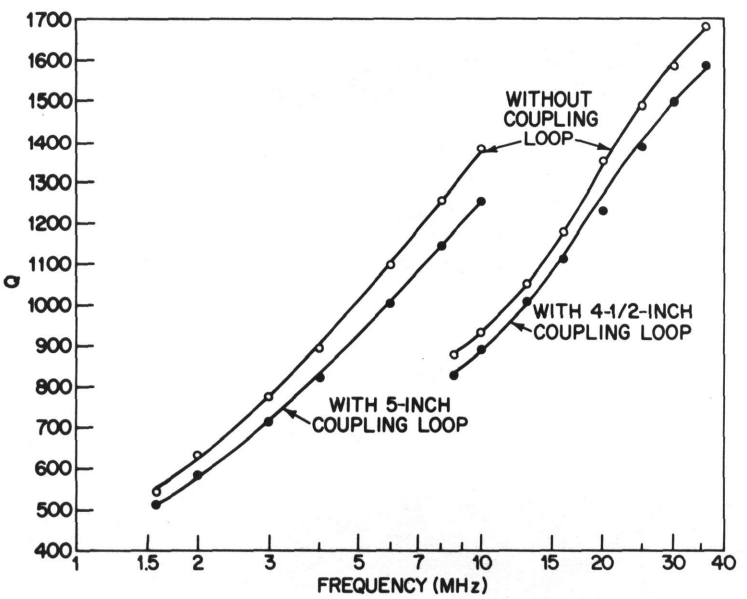

Fig. A11 — Q performance of a more compact arrangement of the inductor described in Fig. A9. The midsection was changed from 2 turns of 1/2-inch tubing to 1 turn of 1/2 inch tubing with 1/2 turn of 1/4-inch tubing with a 1/2-inch pitch on either side.

Fig. A12 — Six-turn inductor from which the Q measurements of Fig. A11 were obtained

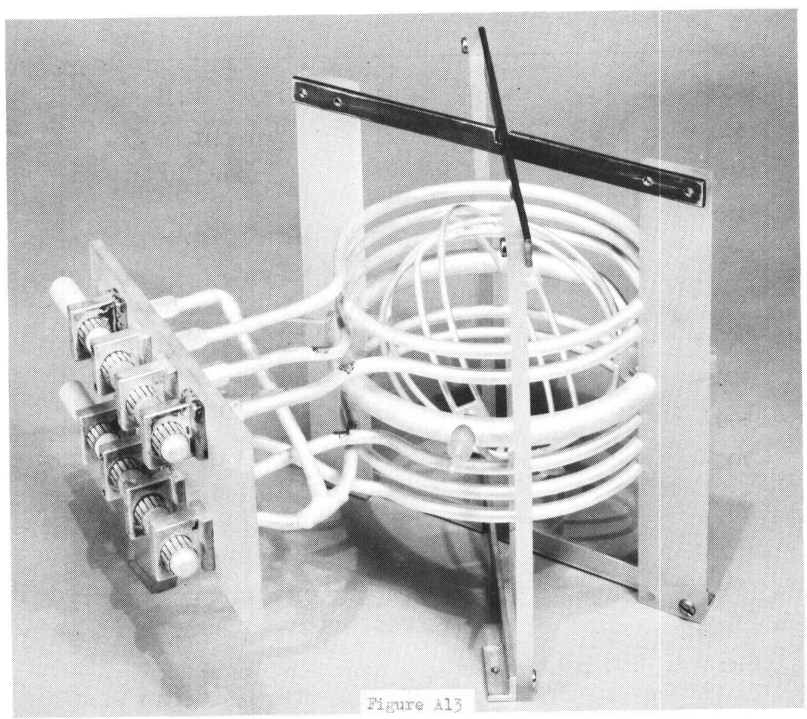

Fig. A13 — Initial band-switching design to change the three-section 6-turn inductor of Fig. A12 from a series connection to a parallel connection

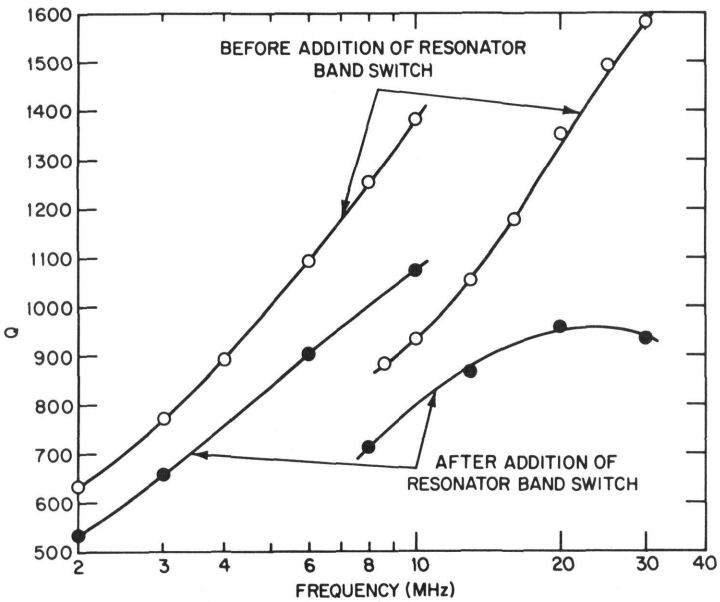

Fig. A14 — Q performance of the initial band-switched-resonator arrangement (Fig. A13)

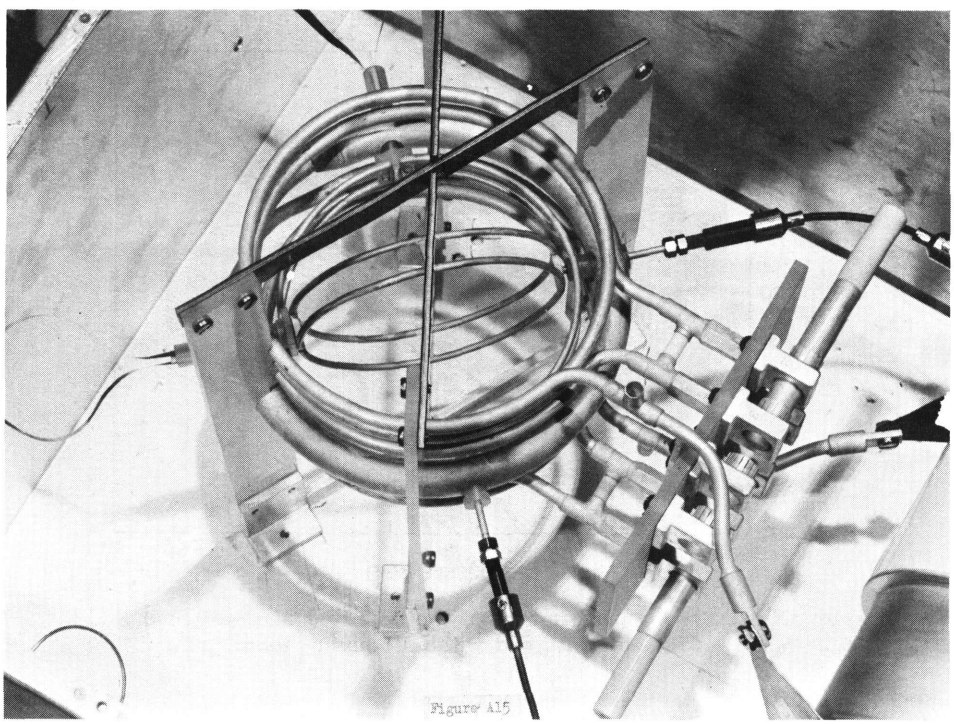

Fig. A15 — Improved band-switching design

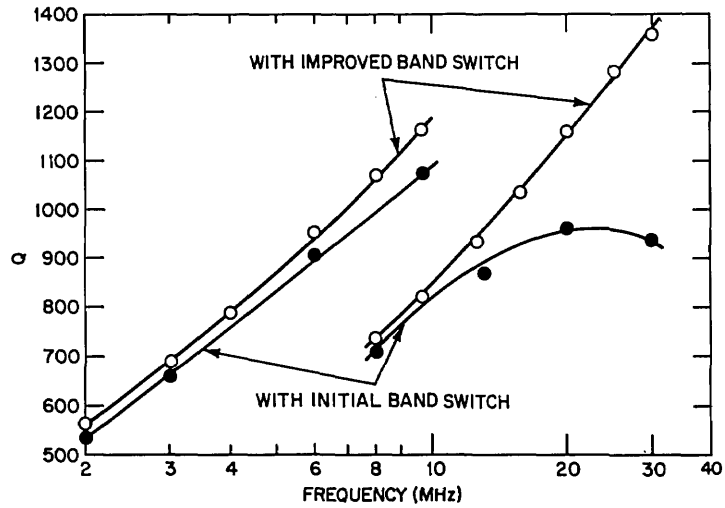

Fig. A16 — Comparison of the Q performance of the improved and the initial band-switched resonator

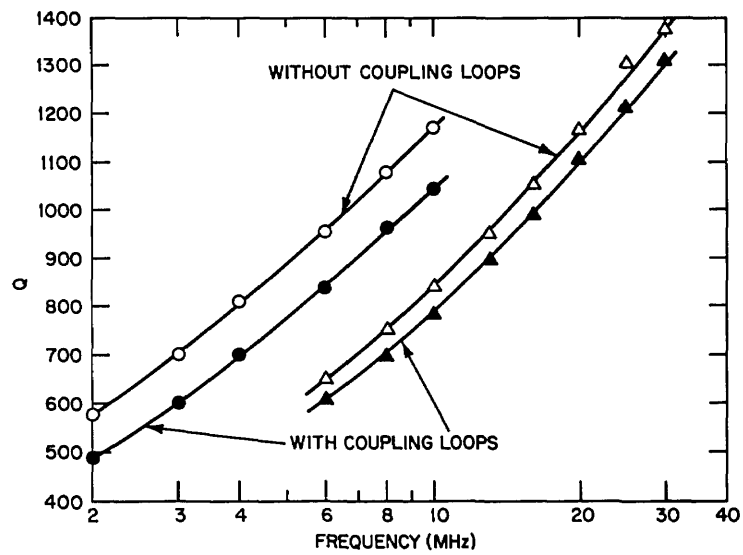

Fig. A17 — Q performance of the improved band-switched resonator with and without coupling loops

Appendix B

DESIGN OF THE RESONATOR AND THE COMBINER

RESONATOR PARAMETERS AND DESIGN OPERATING VALUES

Figure B1 is a simplified schematic diagram for a channel of the SSDS. The input resonator is formed from inductor L_1 and tuning capacitor C_1. The output resonator is formed from inductor L_2 and tuning capacitor C_2. Figures B2 through B4 are useful schematic diagrams in analyzing the channel and developing an equivalent circuit in which all parameters are referred to the mesh containing the input resonator.

In Fig. B2 the load circuit Z_L is replaced by its equivalent in the mesh containing the output resonator. Also, the following reactance notation is assigned elements L_1, C_1, L_2, and C_2:

$$X_1 = \omega L_1, \tag{B1}$$

$$X_2 = 1/\omega C_1, \tag{B2}$$

$$X_3 = \omega L_2, \tag{B3}$$

and

$$X_4 = 1/\omega C_2. \tag{B4}$$

In addition

$$r = \text{resonator loss resistance } X_1/Q \text{ or } X_3/Q \tag{B5}$$

and

$$Z_L = R_L + jX_L \ (X_L \text{ includes the reactance of } L_4). \tag{B6}$$

The resistance (R_1) and reactance (X_5) reflected into the output resonator from the load circuit are

$$R_1 = \frac{(\omega M_3)^2 \, R_L}{R_L{}^2 + X_L{}^2} \tag{B7}$$

and

$$X_5 = -\frac{(\omega M_3)^2 \, X_L}{R_L{}^2 + X_L{}^2}. \tag{B8}$$

Let

$$R_2 = r + R_1. \tag{B9}$$

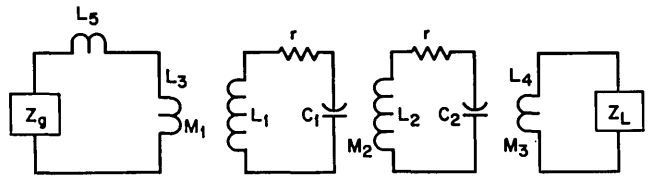

Fig. B1 — Simplified schematic diagram for one SSDS channel with generator and load terminations

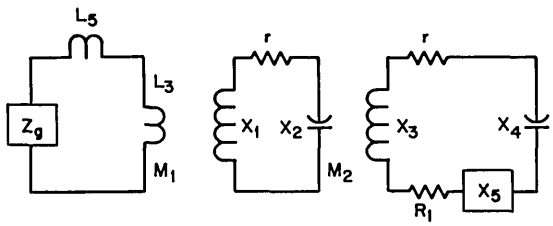

Fig. B2 — Schematic diagram for one channel with the load circuit replaced by its equivalent in the output resonator mesh

Fig. B3 — Schematic diagram for one channel with the output resonator mesh replaced by its equivalent in the input resonator mesh

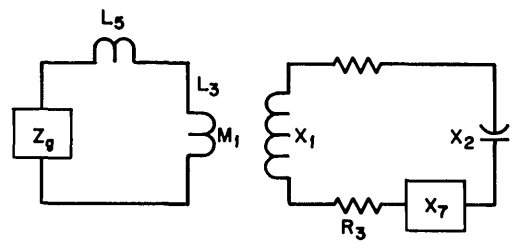

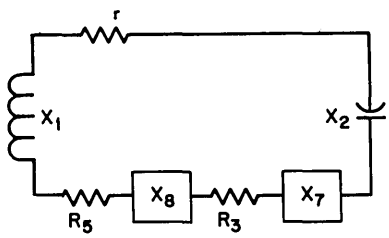

Fig. B4 — Schematic diagram for one channel with all components replaced by their equivalents in the input resonator mesh

The output resonator efficiency e_2 may be defined:

$$e_2 = \frac{R_1}{R_2}. \tag{B10}$$

In Fig. B3 the output resonator is replaced by its equivalent in the mesh containing the input resonator. Let

$$X_6 = X_3 + X_4 + X_5. \tag{B11}$$

Then the resistance (R_3) and reactance (X_7) reflected into the input resonator from the output resonator are

$$R_3 = \frac{(\omega M_2)^2 R_2}{R_2^2 + X_6^2} \tag{B12}$$

and

$$X_7 = -\frac{(\omega M_2)^2 X_6}{R_2^2 + X_6^2}. \tag{B13}$$

Let

$$R_4 = r + R_3. \tag{B14}$$

The input resonator efficiency e_1 may be defined:

$$e_1 = \frac{R_3}{R_4}. \tag{B15}$$

The generator termination Z_g of Fig. B3 is transformed into the mesh containing the input resonator as shown in Fig. B4. Let

$$Z_g = R_g + X_g \text{ (X_g includes the reactance of L_5 and L_3).} \tag{B16}$$

The resistance (R_5) and reactance (X_8) reflected into the input resonator from the generator circuit are

$$R_5 = \frac{(\omega M_1)^2 R_g}{R_g^2 + X_g^2} \tag{B17}$$

and

$$X_8 = -\frac{(\omega M_1)^2 X_g}{R_g^2 + X_g^2}. \tag{B18}$$

In the tuneup procedure an impedance match at the input is achieved, and for this condition

$$R_5 = R_4 \tag{B19}$$

and

$$X_1 + X_2 + X_7 + X_8 = 0. \tag{B20}$$

In the tuneup procedure C_1 is positioned such that Eq. (B20) is satisfied under the condition of zero impedance reflection from the output resonator. Therefore

$$X_7 = 0, \tag{B21}$$

$$X_1 + X_2 + X_8 = 0, \tag{B22}$$

$$X_6 = 0, \tag{B23}$$

and

$$R_3 = \frac{(\omega M_2)^2}{R_2}; \tag{B24}$$

also

$$R_3 = (\omega M_2)^2 \frac{(1 - e_2)}{r}. \tag{B25}$$

Channel transfer efficiency E is the product of the resonator efficiencies:

$$E = e_1 e_2. \tag{B26}$$

From Eqs. (B11) and (B23) the reactance X_4 of output resonator capacitor C_2 can be determined:

$$-X_4 = X_3 + X_5. \tag{B27}$$

From Eq. (B22) the reactance X_2 of input resonator capacitor C_1 can be determined:

$$-X_2 = X_1 + X_8. \tag{B28}$$

The root-mean-square (rms) power loss in the input resonator P_1 is defined as

$$P_1 = P_A(1 - e_1), \tag{B29}$$

where P_A is the channel input power (rms).

The rms power loss in the output resonator P_2 is defined as

$$P_2 = (P_A - P_1)(1 - e_2). \tag{B30}$$

The rms current in the input resonator I_1 is defined as

$$I_1 = \sqrt{P_1/r} \tag{B31}$$

and in the output resonator is defined as

$$I_2 = \sqrt{P_2/r}. \tag{B32}$$

The peak voltage stresses will be imposed under maximum input peak-envelope-power (PEP) conditions. The voltage across the input resonator V_1 is defined as

$$V_1 = 1.414\sqrt{P_p(1 - e_1)QX_1} \tag{B33}$$

and across the output resonator V_2 is defined as

$$V_2 = 1.414\sqrt{P_p e_1(1 - e_2)QX_3}, \tag{B34}$$

where P_p is the peak envelope power (PEP) applied to the channel input in watts.

Figure B5 is a complete schematic diagram for one channel of the SSDS. Subscripts L and H appearing in Fig. B5 designate whether the particular component is appropriate to either the lower (2 to 8 MHz) or the higher (8 to 30 MHz) frequency band. Listed below are element values appropriate to Fig. B5:

$L_{1(L)} = L_{2(L)} = 4.5$ microhenries,
$L_{1(H)} = L_{2(H)} = 0.7$ microhenry,
$L_{3(L)} = L_{4(L)} = 0.3$ microhenry,
$L_{3(H)} = L_{4(H)} = 0.27$ microhenry,
$L_{3(L)} + L_{5(L)} = 1.99$ microhenries,
$L_{3(H)} + L_{5(H)} = 0.358$ microhenry,
K_{max} between $L_{4(L)}$ and $L_{2(L)} = 0.51$ (coefficient of coupling),
K_{max} between $L_{4(H)}$ and $L_{2(H)} = 0.40$ (coefficient of coupling),
$M_{2(L)} = 0.034$ microhenry (mutual coupling),
$M_{2(H)} = 0.0044$ microhenry (mutual coupling),
$M_{3(L)} = K\sqrt{L_{2(L)}L_{4(L)}}$ microhenry (mutual coupling),
$M_{3(H)} = K\sqrt{L_{2(H)}L_{4(H)}}$ microhenry (mutual coupling).

Calculations of the values of the important parameters are provided at various frequencies in Table B1.

COMBINING CIRCUITRY

The ability of a channel to operate into a wide range of termination impedances is defined as its impedance-matching capability (IMC). For a given resonator configuration the IMC of a channel primarily depends on the maximum coefficient of coupling between the output coupling loop and the resonator inductance and on the design value of the output resonator efficiency. Both of these parameters are, to a degree, controllable. The coefficient of coupling K is adjustable by means of mechanical rotation of the output coupling loop. In a practical circuit an upper limit to the maximum achievable value of K is about 0.55. The design value of the output resonator operating efficiency e_2 is primarily established by input and interstage coupling parameters.

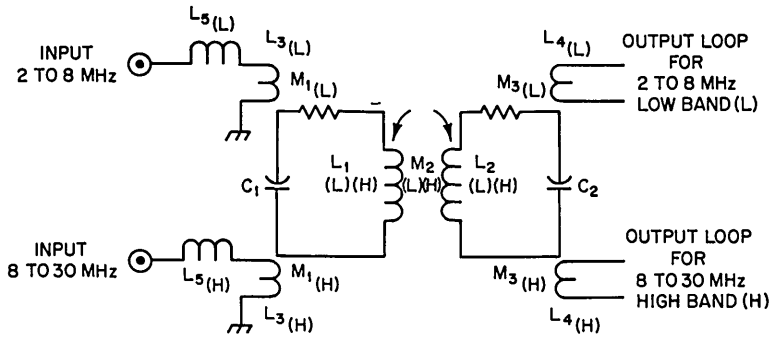

Fig. B5 — Complete schematic diagram for one channel

Table B1

Calculations of pertinent parameters for a single channel. (All rms values are computed for a 1.0-kW-rms input to the channel. All peak values are computed for a 2-kW-PEP (peak-envelope-power) input to the channel. Both conditions are satisfied by a two-tone 2-kW-PEP input.)

Frequency (MHz)	Q	r (ohms)	R_5 (ohms)	R_3 (ohms)	R_2	e_1 (%)	e_2 (%)	E (%)	P_1 (W rms)	I_1 (A rms)	V_1 (kV peak)	P_2 (W rms)	I_2 (A rms)	V_2 (kV peak)
Low Band														
2	470	0.120	0.545	0.425	0.429	78	72	56.3	220	42.8	4.8	218	42.6	4.8
4	670	0.169	1.349	1.18	0.619	87.5	72.8	63.7	125	27.2	6.2	238	37.5	8.5
8	900	0.226	1.966	1.74	0.982	88.5	77	68	115	22.6	9.7	204	30.0	12.9
High Band														
8	640	0.0555	0.309	0.254	0.193	82.2	71.4	58.7	178	56.9	4.0	235	65.4	4.6
16	900	0.078	0.920	0.842	0.232	91.5	66.4	60.7	85	32.97	4.6	307	62.7	8.8
30	1200	0.11	1.72	1.609	0.428	93.6	74.3	69.5	64	24.1	6.4	241	46.8	12.4

Impedance-matching capability can be expressed quantitatively if Eqs. (B7), (B9), and (B10) are combined to relate output resonator parameters and load impedance terms:

$$R_1(1 + q^2) = \omega Q\left(\frac{1 - e_2}{e_2}\right) K^2 L_4, \tag{B35}$$

where $q = X_L/R_L$ and $K = M_3/(L_2L_4)^{1/2}$. The upper limit of the right-hand half of Eq. (B35) is reached when K is at its maximum value K_{max}. Under these conditions the resonator is being operated at its maximum IMC limit, and

$$R_L(1 + q^2) = \omega Q\left(\frac{1 - e_2}{e_2}\right) K_{max}^2 L_4. \tag{B36}$$

If

$$R_L(1 + q^2) < \omega Q\left(\frac{1 - e_2}{e_2}\right) K_{max}^2 L_4,$$

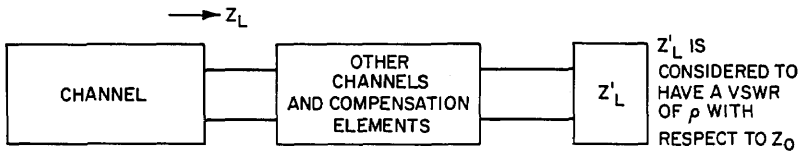

Fig. B6 — Output impedance relationships for one channel

then K is reduced as required. The load impedance term $R_L(1 + q^2)$ is the familiar series-to-parallel resistance transformation. Also, any complex load impedance, when put into the form $R_L(1 + q^2)$, is normalized to an equivalent purely resistive termination insofar as the coupling requirement K is concerned.

From equation (B36) the IMC increases directly with frequency and unloaded Q factor. For a given resonator design operable over a frequency ratio of 4 the IMC should be approximately 8 times larger at the upper frequency limit than at the lower frequency limit. This assumes constant resonator efficiency and a rise in resonator Q factor proportional to the 1/2 power of frequency.

Figure B6 describes output impedance relationships for a channel. The external termination Z_L' is modified by the presence of the coupling loops of the other channels (including interconnection effects) and compensation elements and appears to the channel of interest as impedance $Z_L = R_L \pm jX_L$. Z_L' can be further defined in terms of its characteristic value (Z_0) and a VSWR (ρ) relative to the characteristic value. Let VSWR be unity ($\rho = 1$). Under these conditions the R_L and X_L components of Z_L are the values of the channel's nominal load impedance. R_L and X_L may then be converted to an equivalent impedance-matching-demand (IMD) factor by putting it into the form $R_L(1 + q^2)$. The IMD factor for any value of ρ then becomes

$$\text{IMD} = \rho R_L(1 + q^2). \tag{B37}$$

The objective in the design of the combining circuit is therefore to determine an arrangement of n coupling loops (and their interconnections) together with compensation impedances such that ρ is maximized but consistent with the output resonator parameters. Thus, from Eqs. (B36) and (B37),

$$\rho_{max} = \frac{\omega Q \left(\frac{1 - e_2}{e_2}\right) K_{max}^2 L_2}{R_L(1 + q^2)}. \tag{B38}$$

The numerator is entirely a function of output resonator parameters. The denominator involves the number of channels, their interconnections, and any impedance compensation. In Eq. (B38) the values assigned to R_L and q must be appropriate to the nominal load impedance as previously defined.

Figure B7 is a plot of the cumulative reactance measured for two- and five-loop series-connected loop arrangements. These data show the normal nonlinear relationship of reactance vs frequency because of the effects of distributed capacity. To better account for these effects, the coupling loops together with their interconnections can be considered as a transmission line having characteristic impedance Z_a and being of electrical length θ.

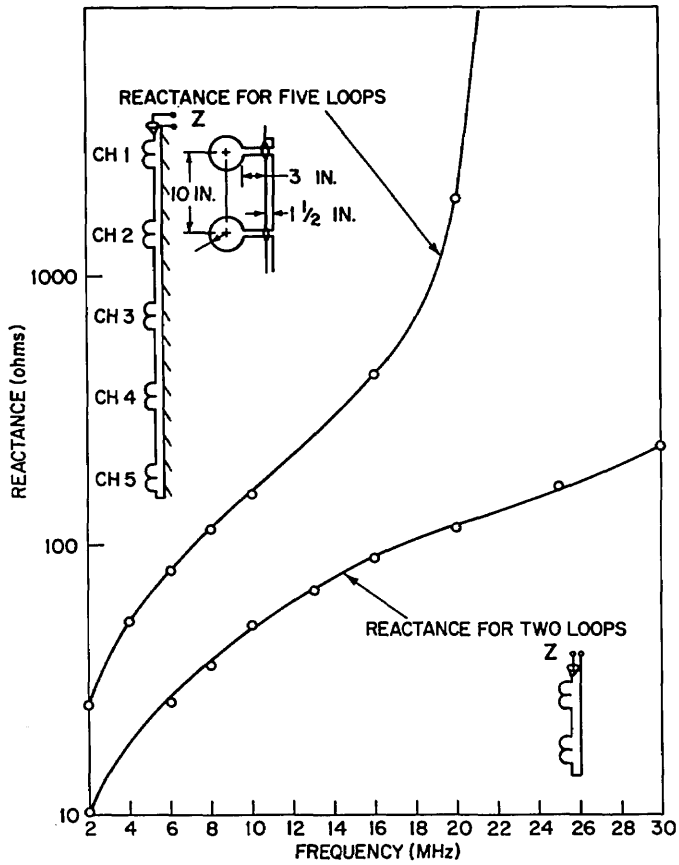

Fig. B7 — Cumulative reactance for SSDS output-coupling-loop arrangements

From input impedance measurements of the coupling-loop arrangements of Fig. B7 the characteristic impedance Z_a has been determined to be approximately 178 ohms. The electrical lengths of the two- and five-loop arrangements are plotted in Fig. B8. The cumulative reactance transformed to the input can then be calculated from normal transmission-line equations.

The combining arrangements used for the low band (2 to 8 MHz) and high band (8 to 30 MHz) are described in Figs. B9 and B10 respectively. These networks were optimized using a computer-aided approach which permitted many combinations of element values to be examined. The calculations have been performed for the channel locations representing worst-case situations. For the low band (2 to 8 MHz) the worst-case channel location is channel 1. For the high band (8 to 30 MHz) the worst-case location is channel 2 or channel 3. Table B2 summarizes the calculations of impedance-matching capability.

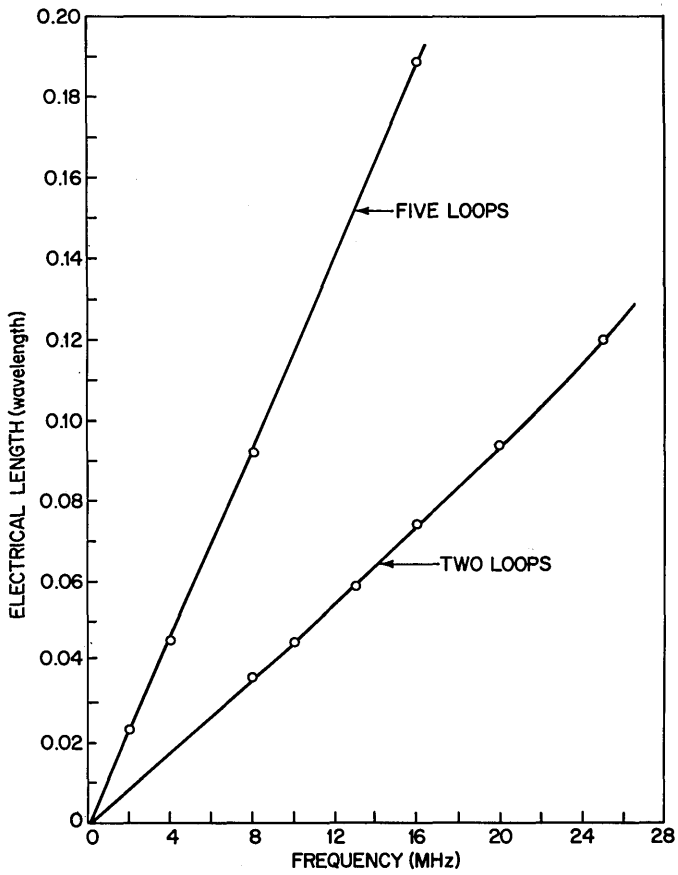

Fig. B8 — Electrical lengths of SSDS coupling-loop arrangements

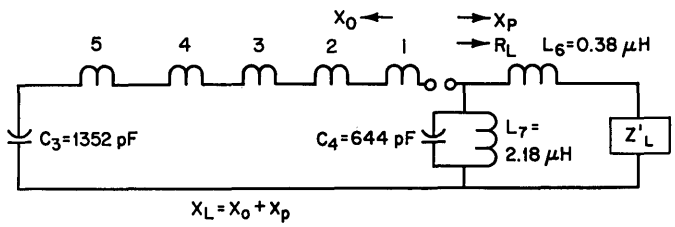

Fig. B9 — Combining arrangement for the low band (2 to 8 MHz)

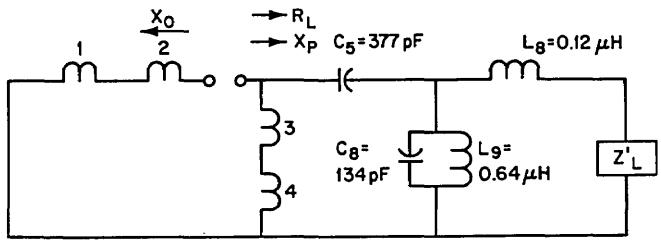

Fig. B10 — Combining arrangement for the high band (8 to 30 MHz)

Table B2
Summary of impedance matching capabilities for the low-band arrangement of Fig. B9 and for the high-band arrangement of Fig. B10. (All calculations for the low band were for the channel 1 position, and all calculations for the high band were for the channel 2 position.)

f_0 (MHz)	R_L (ohms)	X_L (ohms)	ρ (max VSWR)
Low-Band Arrangement			
2.0	15.7	−j 7.0	6.34
3.0	32.4	+j 19.3	5.06
4.0	47.2	+j 36.1	5.10
6.0	49.5	+j 49.0	6.13
8.0	33.3	+j 68.8	4.58
High-Band Arrangement			
8.0	63.7	+j 37.8	4.73
10.0	36.4	+j 54.4	5.40
13.0	35.8	+j 81.3	4.82
16.0	44.1	+j 104.8	4.95
20.0	58.3	+j 129.3	5.60
25.0	69.6	+j 156.7	5.59
30.0	62.7	+j 201.4	3.49

*U.S. GOVERNMENT PRINTING OFFICE: 1974 542-169/Z-200 1-3

Security Classification

DOCUMENT CONTROL DATA - R & D

(Security classification of title, body of abstract and indexing annotation must be entered when the overall report is classified)

1. ORIGINATING ACTIVITY *(Corporate author)* Naval Research Laboratory Washington, D.C. 20375	2a. REPORT SECURITY CLASSIFICATION Unclassified 2b. GROUP

3. REPORT TITLE

A FIVE-CHANNEL (2-kW-PEP) 2 TO 30 MHz DISTRIBUTION SYSTEM

4. DESCRIPTIVE NOTES *(Type of report and inclusive dates)*

An interim report on a continuing NRL Problem.

5. AUTHOR(S) *(First name, middle initial, last name)*

Harold D. Murray, Denis Q. Arnesen, and Charles E. Hobbis

6. REPORT DATE December 21, 1973	7a. TOTAL NO. OF PAGES 46	7b. NO. OF REFS 0
8a. CONTRACT OR GRANT NO. NRL Problem R01-31 b. PROJECT NO. NavElecSysCom XF-14-222-013-K132 c. NavSEC P.O. 1-0070 d.	9a. ORIGINATOR'S REPORT NUMBER(S) NRL Report 7659 9b. OTHER REPORT NO(S) *(Any other numbers that may be assigned this report)*	

10. DISTRIBUTION STATEMENT

Approved for public release; distribution unlimited.

11. SUPPLEMENTARY NOTES	12. SPONSORING MILITARY ACTIVITY Department of the Navy, Naval Electronic Systems Command, Washington, D.C. 20376; Naval Ship Engineering Center, Washington, D.C. 20360

13. ABSTRACT

The concept of a radio-frequency distribution system customized to the special requirements and constraints of ships having five transmitters or less has been investigated. The analysis, experimental design, and measurements of the performance of an experimental model of one channel of the system has successfully been completed. When fully implemented the system will provide for the simultaneous operation of five transmitters in the 2 to 30 MHz frequency range into two broadband antennas in a single systems package. A program should be initiated to develop a complete self-contained selective distribution system as an engineering model of the system whose design was proven by the present investigation.

DD FORM 1 NOV 65 1473 (PAGE 1)

S/N 0101-807-6801

Security Classification

Security Classification

14. KEY WORDS	LINK A		LINK B		LINK C	
	ROLE	WT	ROLE	WT	ROLE	WT
Multicoupler						
Antenna coupling networks						
Transmitter couplers						
RF distribution						
Antenna circuitry						
Telecommunication						
Shipboard communication						
HF communication						

DD FORM 1 NOV 65 1473 (BACK)
(PAGE 2)

Security Classification